ISTANBUL TECHNICAL UNIVERSITY ★ GRADUATE SCHOOL OF SCIENCE ENGINEERING AND TECHNOLOGY

THE EFFECT OF PRODUCTION PARAMETERS ON THE PROPERTIES OF CONTINUOUS GRAPHENE OXIDE FIBERS

M.Sc. THESIS

Mervin ÖLMEZ

Department of Polymer Science and Technology

Polymer Science and Technology Programme

JUNE 2018

ISTANBUL TECHNICAL UNIVERSITY ★ GRADUATE SCHOOL OF SCIENCE ENGINEERING AND TECHNOLOGY

THE EFFECT OF PRODUCTION PARAMETERS ON THE PROPERTIES OF CONTINUOUS GRAPHENE OXIDE FIBERS

M.Sc. THESIS

Mervin ÖLMEZ
(515151035)

Department of Polymer Science and Technology

Polymer Science and Technology Programme

Thesis Advisor: Prof. Dr. H. Ayşen ÖNEN

JUNE 2018

ISTANBUL TEKNİK ÜNİVERSİTESİ ★ FEN BİLİMLERİ ENSTİTÜSÜ

ÜRETİM PARAMETRELERİNİN SÜREKLİ GRAFEN LİF ÖZELLİKLERİ ÜZERİNE ETKİSİ

YÜKSEK LİSANS TEZİ

Mervin ÖLMEZ
(515151035)

Polimer Bilimi ve Teknolojisi Anabilim Dalı

Polimer Bilimi ve Teknolojisi Programı

Tez Danışmanı: Prof. Dr. H. Ayşen ÖNEN

HAZİRAN 2018

Mervin Ölmez, a M.Sc. student of İTU Graduate School of Science Engineering and Technology student ID 515151035, successfully defended the thesis entitled "THE EFFECT OF PRODUCTION PARAMETERS ON THE PROPERTIES OF CONTINUOUS GRAPHENE OXIDE FIBERS", which she prepared after fulfilling the requirements specified in the associated legislations, before the jury whose signatures are below.

Thesis Advisor :	**Prof. Dr. H. Ayşen ÖNEN** İstanbul Technical University	....
Jury Members:	**Prof. Dr. Fatoş Yüksel GÜVENİLİR** İstanbul Technical University	....
	Prof. Dr. Cemal ÖZEROĞLU İstanbul University	....

Date of Submission : 03 May 2018
Date of Defense : 04 June 2018

To my family,

FOREWORD

I would like to thank to my supervisors Professor Dr. H. Ayşen ÖNEN and Professor Dr. Nuray UÇAR for their excellent guidance and support during this process. I am honored to work with them and I am pleased to have an opportunity to benefit from their wide knowledge.

I am grateful of the financial supports and scholarships from The Scientific and Technological Research Council of Turkey (TUBITAK) (Project No: 114M524) and Istanbul Technical University Scientific Research Coordination Unit (ITU BAP) (Project ID: 40709)

It was also great experience to work with my laboratory colleague Özge ALPTOĞA who was always helpful to me. I am very sure that she was the best colleague who I have ever work with.

I extend my appreciation to my friends Emine Sena KAZAN, Dilşa Sinem ÇELİK and Orhan PITIR. When I lost my interest, they kept me motivated and without their support and encouragement, it would be hard to finish this work.

Last but not least, my special thanks go to my lovely parents Aynur and Cengiz ÖLMEZ. From very beginning to the end, they have never spared their love and support. I feel honored for being their daugther.

June 2018

Mervin ÖLMEZ
(Chemical Engineer)

TABLE OF CONTENTS

Page

FOREWORD ix
TABLE OF CONTENTS xi
ABBREVIATIONS xiii
SYMBOLS xv
LIST OF TABLES xvii
LIST OF FIGURES xix
SUMMARY xxi
ÖZET xxiii
1. INTRODUCTION 1
2. THEORETICAL PART 3
2.1 Fiber and Fiber Properties 3
2.1.1 Types of fibers 3
2.1.1.1 Natural fibers 3
2.1.1.2 Artificial fibers 4
2.1.2 Physical and mechanical properties of fibers 4
2.1.3 Chemical properties of fibers 6
2.2 Spinning Techniques 6
2.2.1 Melt spinning 7
2.2.2 Solution wet spinning 8
2.2.3 Solution dry spinning 10
2.2.4 Dry-jet wet spinning 11
2.2.5 Gel spinning 12
2.2.6 Phase separation spinning 13
2.2.7 Reaction spinning 13
2.2.8 Electrospinning 13
2.3 General Properties of Graphene 14
2.3.1 Electronic properties of graphene 15
2.3.2 Mechanical properties of graphene 15
2.3.3 Thermal properties of graphene 16
2.3.4 Fabrication of graphene 16
2.3.4.1 Micromechanical cleavage 16
2.3.4.2 Liquid-phase exfoliation 17
2.3.4.3 Reduction of graphene oxide 18
2.4 Graphene Oxide and Graphene Oxide Fiber 19
2.4.1 Applications of graphene oxide fiber 20
3. EXPERIMENTAL PROCEDURE 23
3.1 Materials 23
3.2 Methods 23
3.2.1 Thermal exfoliation 23
3.2.2 Preparation of graphene oxide dispersion by modified Hummers method 25
3.2.3 Mechanical homogenization and ultrasonication 26

3.2.4 Wet spinning of graphene oxide 27
3.3 Characterization 28
3.3.1 Scanning electron microscopy (SEM) 28
3.3.2 Tex number 28
3.3.3 Electrical conductivity 28
3.3.4 Tensile testing 29
3.3.5 X-ray photoelectron spectroscopy (XPS) 29
3.3.6 Atomic force microscopy (AFM) 29
3.3.7 X-ray diffraction (XRD) 29
4. RESULTS AND DISCUSSION 31
4.1 Scanning Electron Microscopy (SEM) 31
4.2 Tex Number 33
4.3 Electrical Conductivity 34
4.4 Tensile Testing 35
4.5 X-ray Photoelectron Spectroscopy (XPS) 36
4.6 Atomic Force Microscopy (AFM) 40
4.7 X-ray Diffraction (XRD) 43
5. CONCLUSION 45
REFERENCES 49
CURRICULUM VITAE 55

ABBREVIATIONS

2D	**:** 2-Dimensional
AC	**:** Activated Carbon
AFM	**:** Atomic Force Microscopy
CNT	**:** Carbon Nanotubes
CS	**:** Cross Sectional
G	**:** Graphene
GO	**:** Graphene Oxide
HDPE	**:** High Density Polyethylene
L	**:** Longitudinal
LDH	**:** Layered Double Hydroxide
SEM	**:** Scanning Electron Microscopy
rpm	**:** Revolutions Per Minute
XPS	**:** X-ray Photoelectron Spectroscopy
XRD	**:** X-ray Diffraction

SYMBOLS

Å	: Angstrom
A	: Cross sectional area of sample
e	: Extension
ε	: Strain
E	: Young's modulus
GPa	: Gigapascal
K	: Kelvin
l	: Stretched length
l_o	: The original length
MPa	: Megapascal
N	: Newton
nm	: Nanometer
Pa	: Pascal
σ	: Stress
V	: Voltage

LIST OF TABLES

Page

Table 3.1 : Sample codes **27**
Table 3.2 : Coagulation baths... **28**
Table 4.1 : Tex numbers.. **34**
Table 4.2 : Electrical conductivity **35**
Table 4.3 : Tensile properties.. **36**
Table 4.4 : Elemental compositions... **36**
Table 4.5 : Binding energies and percentages... **37**
Table 4.6 : AFM results of samples **40**
Table 4.7 : XRD results of samples **43**

LIST OF FIGURES

Page

Figure 2.1 : Classification of fibers.......... **3**
Figure 2.2 : Melt spinning.......... **7**
Figure 2.3 : Wet spinning.......... **9**
Figure 2.4 : Dry spinning.......... **10**
Figure 2.5 : Dry jet wet spinning.......... **11**
Figure 2.6 : Gel spinning.......... **12**
Figure 2.7 : Electrospinning.......... **13**
Figure 2.8 : Micromechanical cleavage.......... **17**
Figure 2.9 : Liquid-phase exfoliation.......... **18**
Figure 2.10 : Reduction of GO [27].......... **18**
Figure 3.1 : Fixed-bed tube oven.......... **23**
Figure 3.2 : Relatively fish tail part and lid part of quartz tube.......... **24**
Figure 3.3 : Graphene, before exfoliation step.......... **24**
Figure 3.4 : Graphene, after exfoliation step.......... **25**
Figure 3.5 : Mixture, before the addition of hydrogen peroxide.......... **25**
Figure 3.6 : Mixture, after the addition of hydrogen peroxide.......... **26**
Figure 3.7 : Mixture, before the addition of hydrogen peroxide.......... **28**
Figure 4.1 : SEM micrographs of 1050C-35s referenced sample, CS, L.......... **31**
Figure 4.2 : SEM micrographs of 1020C-45s referenced sample, CS, L.......... **31**
Figure 4.3 : SEM micrographs of 1000C-15s referenced sample, CS, L.......... **31**
Figure 4.4 : SEM micrographs of 1000C-35s referenced sample, CS, L.......... **32**
Figure 4.5 : SEM micrographs of 1000C-35s-Ult-S referenced sample, CS, L.......... **32**
Figure 4.6 : SEM micrographs of 1000C-35s-Ult-L referenced sample, CS, L.......... **32**
Figure 4.7 : SEM micrographs of 1020C-35s referenced sample, CS, L.......... **32**
Figure 4.8 : SEM micrographs of 1020C-35s-AC referenced sample, CS, L.......... **33**
Figure 4.9 : XPS graph of 1000C-15s.......... **37**
Figure 4.10 : XPS graph of 1000C-35s.......... **38**
Figure 4.11 : XPS graph of 1000C-35s-Ult-S.......... **38**
Figure 4.12 : XPS graph of 1000C-35s-Ult-L.......... **38**
Figure 4.13 : XPS graph of 1020C-35s.......... **39**
Figure 4.14 : XPS graph of 1020C-45s.......... **39**
Figure 4.15 : XPS graph of 1050C-35s.......... **39**
Figure 4.16 : AFM profile of 1000C-15s.......... **40**
Figure 4.17 : AFM profile of 1000C-35s.......... **41**
Figure 4.18 : AFM profile of 1000C-35s-Ult-S.......... **41**
Figure 4.19 : AFM profile of 1000C-35s-Ult-L.......... **41**
Figure 4.20 : AFM profile of 1020C-45s.......... **42**
Figure 4.21 : AFM profile of 1050C-35s.......... **42**
Figure 4.22 : AFM profile of 1020C-35s.......... **42**

THE EFFECT OF PRODUCTION PARAMETERS ON THE PROPERTIES OF CONTINUOUS GRAPHENE OXIDE FIBERS

SUMMARY

Graphene is carbon-based material that has promising properties for different applications in energy, catalysts, radar absorber, sensor, etc. Due to its fascinating facilities, this material has been studied by many researchers. By these knowledges, continuous graphene fibres have been fabricated by wet-spinning method and co-coagulants processes have been employed respectively. Because of the excellent properties such as mechanical, thermal, chemical, electrical and economical properties it can be used for low cost production, easy processing with high yield. Graphene (G) is the material which is type of graphite with single layer. Visual properties of G is different from other carbon based materials. It has a 2-dimensional (2D) honeycomb structure and has sp2- bonded carbon atoms in its structure. There are several methods to obtain graphene. It can be directly obtained from graphite or may be obtained from reduction of graphene oxide (GO). Graphene oxide is obtained by the oxidation of graphite by different methods such as Brodie, Hummers or Staudenmaier. Among these, the most common method is Hummers method. The exfoliated GO sheets are highly oxidized and featured with the residual epoxides, hydroxides and carboxylic acid groups on their surfaces.

This study reports the effect of processing parameters such as time, temperature of the exfoliation together with dispersion preparation methods of graphene oxide on the properties of continuous graphene oxide fibers produced by coagulation bath. Relationship between changing parameters and structural properties of graphene oxide fiber, fiber morphology, roughness, crystalline structure have been discussed. Higher exfoliation time leads to an increase in Tex count of fiber, while longer ultrasonic times resulted in lower tex count compared to both shorter ultrasound time and mechanical homogenization. Shorter ultrasonication period and shorter exfoliation time leads to higher electrical conductivity compared to mechanical homogenization. Shorter ultrasonication period results in slight tendency of an increase in breaking strength. Besides, the effect of exfoliation time and presence of activated carbon particle (AC) on graphene oxide fiber's properties has been analyzed. It has been seen that cross-sectional appearance of sample with AC is grating and rough because of AC. The addition of AC did not change the electrical conductivity. However, AC results in an enormous decrease in the mechanical properties. In the light of this study, optimal conditions for producing continuous graphene oxide fibers can be determined. This study can take an important role for further researches.

ÜRETİM PARAMETRELERİNİN SÜREKLİ GRAFEN LİF ÖZELLİKLERİ ÜZERİNE ETKİSİ

ÖZET

Lifler, çapının veya genişliğinin en az 100 katı uzunluğa sahip olan ve doğal bazlı veya üretilmiş olabilen bir malzemedir. Lifler, doğal ve sentetik elyaf olarak iki genel kategoriye ayrılır. Doğal lifler kökenine göre bitki, hayvan veya mineral bazlı olarak sınıflandırılabilir. Bitki bazlı lifler doğada kaybolabilme özelliğinden dolayı çevre dostudur. Hayvansal liflerden en çok kullanılanları ipek ve yündür. Bu sınıfa giren lifler tekstil sektöründe oldukça yoğun kullanılabilmektedir. Mineral liflere de asbest örnek verilebilir.

Sentetik lifler, organik ve inorganik hammaddelerden kimyasal işlemlerle üretilir. Ayrıca bu lifler selüloz gibi doğal liflerin işlenmesi ile de üretilebilir. En çok kullanılan sentetik liflere örnek olarak polietilen, polipropilen, naylon verilebilir. Lifler fiziksel, mekanik ve kimyasal özellikleri ile karakterize edilebilir. Fiziksel özellikleri açısından değerlendirildiğinde liflerin L/D oranları önem taşımaktadır.

Özelliklerine göre lifler farklı eğirme teknikleri ile üretilebilir. Eriyik eğirme yöntemi, ıslak eğirme yöntemi, kuru çekim yöntemi, kuru-jet çekim yöntemi, jel çekim yöntemi, faz ayrımı yöntemi, reaksiyon eğirme yöntemi, electrospinning yöntemi ayrı ayrı açıklanmış, avantaj ve dezavantajlarına değinilmiştir. En çok kullanulan yöntemler çalışmada listelenmiştir. Bu çalışmada ıslak eğirme yöntemi esas alınmıştır.

Karbon ve karbon bazlı malzemeler doğada önemli bir rol oynamaktadır. Elektriksel özellikleri, kimyasal yapıları ve ısıl özellikleri bakımından karbon bazlı ürünler araştırmacılar tarafndan oldukça detaylı incelenmiştir. Grafen de karbon bazlı malzemeler ailesinin bir üyesidir. Günümüzde grafen çoğu araştırmacı tarafından ele alınan, oldukça geniş kullanım alanına sahip bir materyaldir. Araştırmalarda bu denli yoğun kullanılmasının başlıca nedenleri arasında; kolay işlenebilirliği ve düşük maliyeti ile birlikte yüksek verime sahip olması yer almaktadır. Grafen bu üstün özellikleri sayesinde pillerde, süperkapasitörlerde, yakıt hücreleri gibi enerji uygulamalarında yaygın olarak kullanılmaktadır. Bu uygulamaların yanı sıra; biyolojik uygulamalarda, kompozitlerde, optik uygulamalarda da kullanımı mevcuttur. Grafenin kolay işlenebilme özelliğinden yararlanılarak lif üretimi gerçekleştirilmiştir. Grafen ilk olarak 2004 yılında elde edilmiştir. Elde edilmesi sırasında özel ekipmana ihtiyaç duyulmamıştır. Yapışkan bantın grafit yüzeyinden çekilmesi işlemi ile tek tabaka grafen elde edilebilmiştir. Çok tabakalı grafen eldesi için ise işlem tekrarlanmıştır. Bu işlemin kesikli ve küçük ölçekli olması sebebiyle grafen elde etmek için farklı yöntemler denenmiştir. Bunlar arasında en önemlileri sıvı faz eksfoliasyonu yöntemi ve grafen oksitin indirgenmesi yöntemidir. Geliştirilen bu yöntemlerle büyük ölçekli üretimlere olanak sağlanmıştır.

Grafen, grafitin tek tabakalı hali olarak tanımlanabilir. 2 boyutlu (2D) bir petek yapısının görünüşüne sahiptir ve yapısında sp2-bağlı karbon atomlarını ihtiva eder. Grafitten direkt olarak veya grafen oksidin indirgenmesi yolu ile elde edilebilir. Grafen

oksit, grafitin Brodie, Hummers veya Staudenmaier gibi farklı yöntemlerle oksitlenmesiyle elde edilir. Bu yöntemler arasında en yaygı yöntemlerden biri Hummers yöntemidir ve bu çalışmada da Hummers yöntemi esas alınmıştır. Eksfoliye olmuş grafen oksit tabakaları, yüksek oranda oksitlenir ve yapısında bulunan epoksi, hidroksi ve karboksilik gruplar sayesinde karakterize edilebilir.

Tez konusu olan çalışma temelde üç aşamadan oluşmaktadır. Öncelikle termal olarak ekfoliasyon işlemi uygulanmaktadır. Isıl işlem uygulamasının sonrasında Hummers yöntemi esas alınarak kimyasal işlem yapılmıştır. En son da ıslak eğirme yöntemi kullanılarak lif eldesi sağlanmıştır. Islak eğirme sırasında farklı banyolar kullanılmuştır. Üç temel işlem sırasında değiştirilen süreç değişkenlerinin grafen oksit liflerinin son özellikleri üzerine etkileri incelenip yorumlanmıştır. Eksfoliasyon süresi, sıcaklığı, ultrasonifikasyon uygulaması eklenmesi ve aktif karbon katkılanması gibi yöntemlerle parametreler değiştirilmiştir. Elde edilen liflerin yüzey özellikleri, mukavemetleri, kristal yapıları ayrı ayrı kıyaslanarak yorumlanmıştır.

Öncelikle SEM görüntüleri alınan numunelerin yüzey özellikleri hakkına fikir sahibi olunmuştur. Yüzey özellikleri ayrıca AFM analizi ile de yorumlanmış ve iki analizin sonuçları kıyaslanarak değerlendirirlmiştir. Mekanik özelliklerin belirlenmesi ve kıyaslanması için mukavemet değerleri listelenmiştir. Analizler sonucunad en mukavim referanslı ürün belirlenip aktif karbon ilavesi bu numuneye yapılmuştır. Üretim parametrelerinden homojenizasyon aşaması sırasında farklı homojenizasyon teknikleri kullanılmıştır. Mekanik homojenizasyon ve ultrasonik homojenizasyon teknikleri ayrı ayrı numunelere uygulanmıştır. Ultrasonik homojenizasyon işleminin son ürün üzerine etkilerinin incelenmesinde ultrasonikasyon süresi de hesaba katılmıştır ve farklı sürelerde işlem tekrarlanmıştır.

Eksfoliasyon süresinin artması, lifin Tex sayısında bir artışa neden olurken, daha uzun sürede ultrasonikasyon uygulaması, daha kısa ultrason süresi ve mekanik homojenizasyona kıyasla daha düşük bir Tex değeri elde edilmesine neden olmuştur. Daha kısa süreli ultrasonikasyon uygulamasının ve daha kısa eksfoliasyon süresinin, mekanik homojenizasyona kıyasla daha yüksek elektrik iletkenliğine yol açtığı gözlemlenmiştir.

Ayrıca aktif karbon ilavesinin de lif üzerine etkileri incelenmiş ve aktif karbonun grafen lifi yüzey görünümünü pürüzlü ve gözenekli hale getirdiği gözlemlenmiştir. Aktif karbon katkınlanması elektrik iletkenliği üzerine etki etmezken, mekanik özellikleri oldukça olumsuz ektilediği görülmektedir.

Mekanik özelliklerin yanısıra liflerin karbon ve oksijen yüzdeleri analiz yöntemleri ile belirlenmiştir. Bu analize göre ultrasonikasyon işleminin uzun süreli yapıldığı zaman bazı zayıf bağları kırdığı ve kırılan bu zayıf bağların yarattığı boşluklara serbest oksijenin bağlandığı ve C/O oranında düşme yaşandığı gözlemlenmektedir.

XRD analizi kullanılarak liflerin kristal yapıları incelenmiştir. Kristal yapılarındaki değişiklikler diğer analiz yöntemleri ile kıyaslanarak yorumlanmıştır. Tüm analiz yöntemleri ve numune özellikleri bir arada düşünülerek ileriki çalışmalarda izlenecek yol bu sonuçlara göre belirlenmiştir.

Bu çalışmanın ışığında, ileriki çalışmalarda lif mukavemetinin arttırılması adına en uygun parametreler seçilecek ve uygulama alanına bağlı olarak kullanıma sunulacaktır. Uygulama alanına göre son ürün özellikleri incelenecek vee n uygun özelliklere sahip olan numune referansı belirlenerek çalışmalara ışık tutulacaktır. Yapılan tüm çalışmalar sonucunda üretimi yapılan grafen oksit lifleri yüzey adsorpsiyon çalışmaları, iletken lif çalışmaları, sensor ve enerji uygulamaları gibi bir çok uygulamada kullanılabilmektedir.

1. INTRODUCTION

Fiber is a material which has a length at least 100 times its diameter or width and it can be natural based or manufactured. Fibers are subdivided into two general categories which are natural and synthetic fibers. Natural fibers are obtained from natural sources which are plants, animals or minerals. Synthetic fibers are manufactured from organic and inorganic raw materials via chemical process. Fibers can be characterized by their physical, mechanical and chemical properties. According to their properties, fibers can be manufactured by several spinning techniques. Different spinning techniques can be used for different polymer types. Melt spinning do not have limitations respectively. Because of this reason, it can be used for most of commercial polymers. However, some polymer types are suitable for processing with melting step but some of them is not suitable for this step. Solution wet spinning is another method for producing fine fibers. In this study, wet spinning was used for fiber formation. During the process, by a gear pump, polymer solution is pumped into a solution which is called coagulation bath. At the end of the process, filaments are collected as desired thickness. Usage of different bath compositions causes final products which have different properties. Wet spinning method is easy and useful technique to produce graphene oxide fiber.

Graphene is a carbon-based material that has a honeycomb lattice which has 2D structure. Researchers and industrialists have been fascinated by graphene due to its excellent properties, nowadays it is being frequently studied for supercapacitors, solar cells, composite production, etc.

Graphene oxide is obtained by the oxidation of graphite by different methods such as Brodie, Hummers or Staudenmaier. Among these, the most common method is Hummers method. In this study, Hummers method is used for production of graphene oxide.

General principle of continuous fiber production consists of three main steps:

1) Oxidation of graphite which is sometimes exfoliated by high temperature heating process,

2) The dispersion in suitable solvents such as water in order to disperse and separate the flakes from each other,

3) The coagulation of GO dispersion in suitable coagulation bath in order to obtain continuous GO fiber

Graphene oxide fibers have very large application area and it is investigated detaily in following sections.

2. THEORETICAL PART

2.1 Fiber and Fiber Properties

Generally, fiber is material which has a length at least 100 times its diameter or width and it can be natural or manufactured. Some methods including weaving, knitting, twisting and felting can be used for producing textile fiber. Spinning into yarn process needs requirements, for instance; flexibility, strength, fineness, uniformity, durability and cohesiveness. [1]

2.1.1 Types of fibers

Fibers are subdivided into two general categories which are natural and synthetic fibers. Detailed classification can be seen at Figure 2.1.

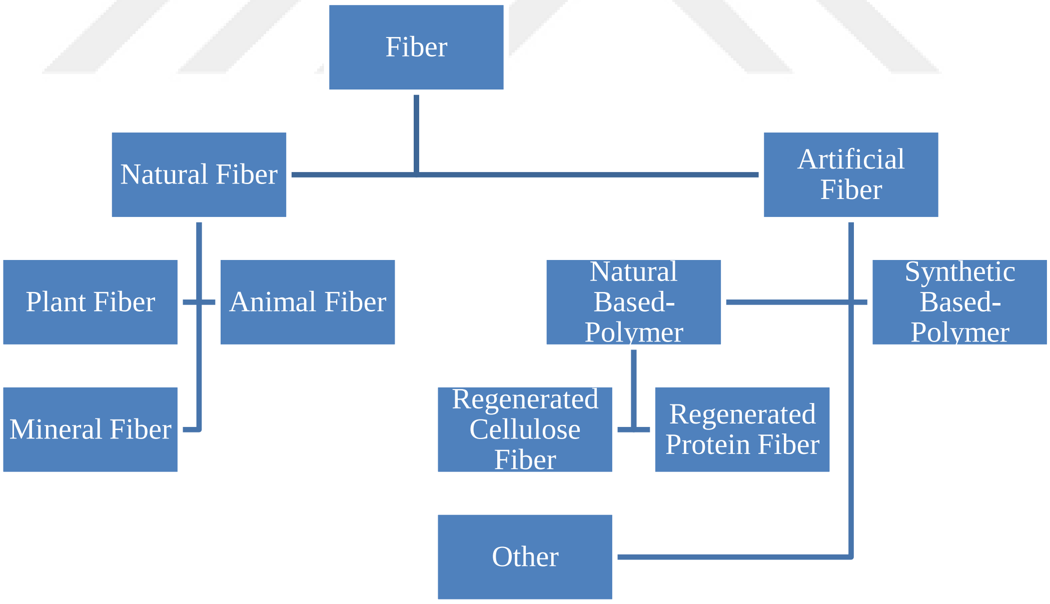

Figure 2.1 : Classification of fibers

2.1.1.1 Natural fibers

Natural fibers are obtained from natural sources which are plants, animals or minerals. Origins determines their class.

Most common plant fibers are cellulose, cotton, jute. Availability and accessibility of natural plant-based fibers are major reasons for an emerging new interest in technology. They are also biodegradable and sustainable raw materials. Nowadays, green technology has took an attention on it and due to its good properties plant-based fibers are used in many areas.

Animal-based fibers are generally proteins. Spider silk, silkworm silk, sinew, catgut, wool is in this class, besides they also have very large usage area in textile industry. Silk fibers are made from cocoons and the fiber has great moisture absorption-desorption, heat retention and staining properties. Wool has also good heat retention property and besides, it is heat insulator.

Asbestos is one of the well-known mineral fiber. It is soft and flexible, moreover it is resistant to heat, electricity and chemical corrosion.

2.1.1.2 Artificial fibers

These fibers are manufactured from organic and inorganic raw materials via chemical process. They also can be natural based like cellulose. Synthetic-based fibers have huge usage area and they can be made from polyethylene, polypropylene, polyurethanes etc.

Synthetic fibers are used in this study. Therefore, synthetic fiber properties and production techniques are examined in the following sections.

Fibers can be utilized in several applications and they are characterized by their physical, mechanical and chemical properties.

2.1.2 Physical and mechanical properties of fibers

Key properties of fiber as physical and mechanical aspect are their morphological appearance, density, thermal and electrical conductivity, extensibility and density. Aspect ratio is the ratio of length to diameter of a fiber and this value is very important as morphological property. It gives a characteristic to the fiber material.

Density is also very notable because fibers can be made of a large variety of materials and individually they have different characteristics. To know density of material can be vital for characterizing of fiber.

Except from density, linear density is more significant for fibers. It refers to the mass per unit length expressed as grams per 9000 or 10000 m of fiber which is called denier.

Tex is also a unit for determining linear density of fiber. It is defined as weight in grams of 1 km of fiber.

Electrical conductivity is another issue in this case. This property is mainly due to fibers desirable properties in terms of electrostatic discharge and resistivity. [1]

Mechanical properties are vital for fibers because they describe fiber characteristics. It is important how the fiber reacts when the fibers face with force such as bending, stretching or twisting. To determine fiber characteristics, several methods have been used by researchers.

Tensile testing is a fundamental method for material science in which a sample is exposed to a controlled tension until failure. Terms of tensile stress, tensile strain, elongation, young's modulus explain fiber behavior when the force is applied. Tensile stress can be described as the resistance to deformation developed within a sample exposed to tension by external force. Units of stress can be Nm^{-2} or Pa.

σ: Stress *(Nm^{-2})*

F: Force applied *(N)*

A: Cross sectional area of sample *(m^{-2})*

$$\sigma: \frac{F}{A} \tag{2.1}$$

Tensile strain can be described as extension per unit length. Strain does not have a unit because it is a ratio of lengths.

ε: Strain

l_o: The original length (m)

e: extension *($l - l_o$) (m)*

l: stretched length (m)

$$\varepsilon: \frac{e}{lo} \tag{2.2}$$

Young's modulus, *E*, is the ratio of change in stress to change in strain within the elastic limits of the material. *E* can be determined by drawing of stress-strain graph. The slope of stress-strain graph gives material's *E* value. Unit of Young's modulus can be Nm^{-2} or Pa.

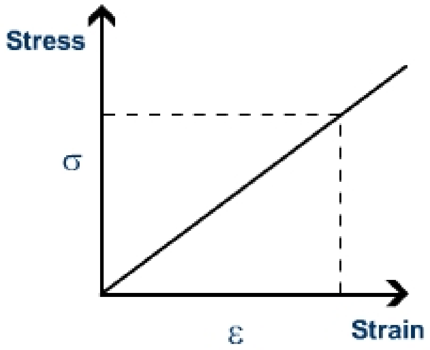

E: Young's Modulus *(Nm^{-2})*

σ: Stress *(Nm^{-2})*

ε: Strain

$$E: \frac{\sigma}{\varepsilon} \tag{2.3}$$

2.1.3 Chemical properties of fibers

Fibers have huge surface area due to its length and they can exhibit functional groups in their structure, therefore these properties give design flexibility to researchers. Several applications can be used for differing fiber properties. Absorption of water, chemical reactivity and solubility are important parameters to understand fiber behavior.

Physical, mechanical and chemical properties specify method of manufacturing of fibers. In next section, fiber forming methods are examined.

2.2 Spinning Techniques

Different spinning techniques were developed for natural and synthetic fiber. Natural fibers can be wool, cotton, silk, jute, etc. Synthetic fibers can be made of polyesters, polyamide, polypropylene, polylactic acid and so on. [2] Different raw materials have specific properties and due to their features, varied processing techniques can be used. Polymers can be converted into continuous filaments. If the polymer is thermoplastic, mostly melting is used for having fiber shape. On the other hand, if polymer cannot be melted or dissolved directly, different methods must be used. There are some requirements for fiber-forming process.

2.2.1 Melt spinning

Melt spinning is one of the well-known fiber manufacturing method among other methods due to its economical properties. This technique is commonly used for synthetic fibers such as nylon, polypropylene, polyester etc. Generally, large spinning towers are used for this process. Process is performed on a large spinning tower. There are metering pump and filtering system to assist the process. Polymer goes down by pump to a metal die. This die contains several number of microscopic holes. By this way, thin polymer strands can be produced. Process continues with cooling operation. This operation is occurred by a cold air blower which rapidly cools and solidifies the strands. After all, some mechanical processes are done such as stretching, crimping, heat setting, etc. [1,2]

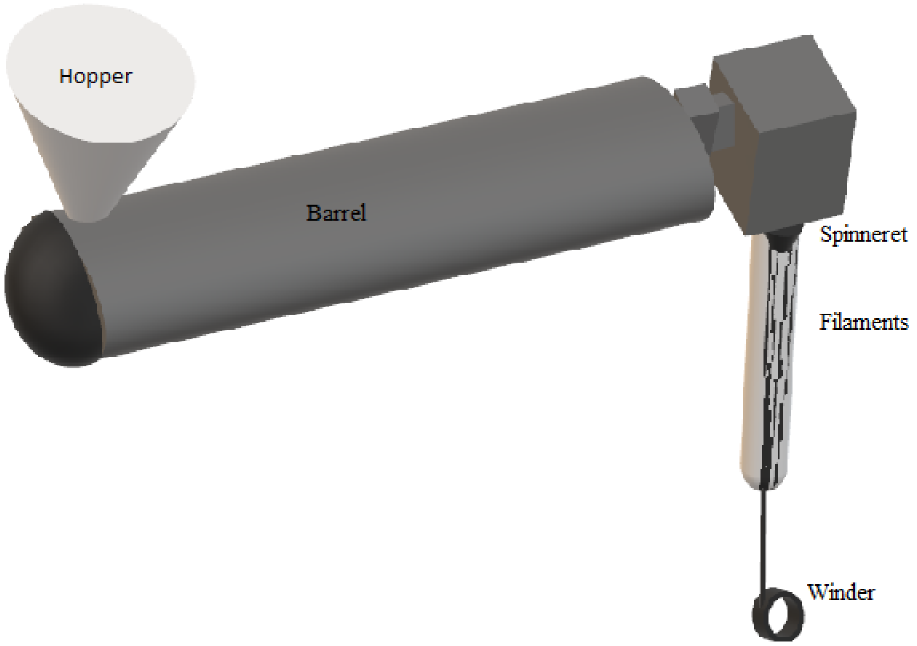

Figure 2.2 : Melt spinning

Melt spinning do not have limitations respectively. Because of this reason, it can be used for most of commercial polymers. Researchers have flexibility to develop this method easily. Some of these developments are discussed below briefly. In a study conducted by Miller *et al.* (2017), feasibility of achievement melt-processible polyacrylonitrile copolymer precursors for producing high strength carbon fibers were examined. Potential of high molecular weight poly(acrylonitrile-ran-methyl acrylate) copolymer was determined by stability dependence on temperature and shear rate. Miller *et al.* reported that poly(acrylonitrile-ran-methyl acrylate) copolymer melt shows strong temperature dependence but does not show a strong dependence on shear-rate according to isothermal DSC and pressurized capillary rheometric experiments. [3]

Kutlu *et al.* (2013) reported melt-spinning of layered double hydroxide (LDH)/high density polyethylene (HDPE) nanocomposites, firstly. According to the report myristic acid modified LDH/HDPE nanocomposite shows the highest exfoliation degree among the experiment which were examined in the study. It is confirmed with semi-quantitative and quantitative rheological models. [4]

Ding *et al.* (2016) investigated thermoelectric properties of n-type Cd doped $PbTeCd_x$ alloys. Melt spinning and hot pressing were used to obtain samples to determine the final properties. As a result of this study, a high-power factor of ~ 42 μW cm^{-1} K^{-2} at 323 K was achieved in n-type $PbTeCd_{0.02}$ with a peak ZT of 1.5 at 773 K as well as an average ZT of 0.93. According to the study, they reported that this achievement of the study is related with the special nanostructures which provide 2DEGs at the coherent interface. [5]

Tomisawa *et al.* (2017) examined the effect of melt spinning conditions on one of the most commonly used synthetic fiber which is polyethylene terephthalate (PET). They reported that a clear difference causes differences in tensile strength and thermal shrinkage of the material that is used. In the study, simultaneous WAXD/SAXS measurements were used to report differences. Several spinning speeds which were 500 to 2000 m/min were applied during spinning process and samples were examined. Consequently, at same conditions crystallites were mainly formed by the phase separation of the fibrillar smectic phase for the fibers spun at 500–1500 m/min, while they mainly developed from the oriented nuclei formed in the spinning process for the fibers spun at 2000 m/min. [6]

2.2.2 Solution wet spinning

Solution wet spinning is another method for producing fine fibers. By a gear pump, polymer pump into a solution which is called coagulation bath. In coagulation bath, polymer precipitates to form filaments. At the end of the process, filaments are collected as desired thickness. Residual solvent is washed and removed by drying process of filaments. [1] Relatively lower speeds are used in wet spinning compared to melt or dry spinning techniques. High tension is observed as a result of using fluids

of higher viscosity. Using of different bath compositions causes final products which have different properties.
Wet spinning was firstly used for manufacturing of rayon by extruding the alcoholic solution of the cellulose nitrate through a mouthpiece dipped in cold water. [7]

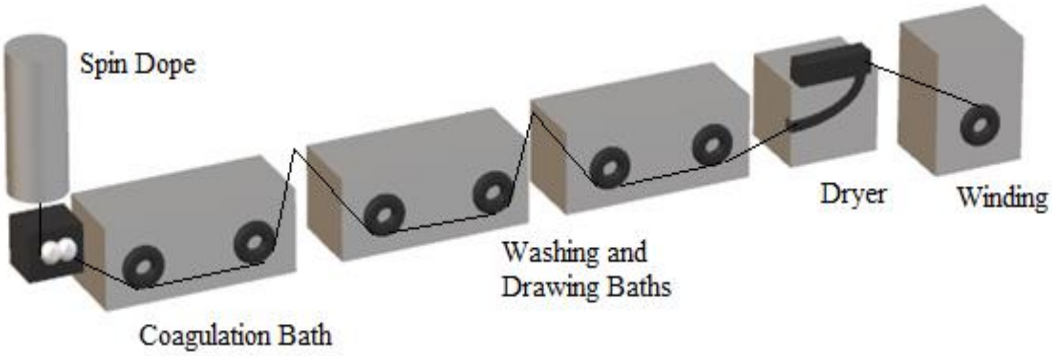

Figure 2.3 : Wet spinning

Many researchers focus on this method and find different ways to improve final products properties.
Lin *et al.* (2016) used wet spinning method to produce graphene fiber. Graphene-based materials have good thermal conductivity. In their study, they examined graphene's thermal transport properties. It is suggested that thermal diffusivity of graphene fibers was at (2.0–2.08) $\times 10^{-6}$ m^2 s^{-1}, and the corresponding intrinsic thermal conductivity was 1.14–1.18 W/m K. Results of this study can be valuable for thermal energy applications. [8]
Nowadays electronic textile applications are well-received and by wet spinning method it can be produced some fibers which are used in this area. Foroughi *et al.* (2016) synthesized polypyrrole containing no substituent on polypyrrole ring by wet spinning. The ultimate tensile strength, elastic modulus and elongation at break of the examined fibers were 25 MPa, 1.5 GPa and 2%, respectively, with an electronic conductivity of ∼3 S/cm. [9]
Mo *et al.* (2018) combined graphene's and polypyrrole's properties to have high-performance fiber-shaped material. In their study a high-performance cellulose nanofibers reinforced graphene/polypyrrole microfiber is fabricated by a convenient wet-spinning method. Fiber that was produced had excellent tensile strength with 364.3 MPa. And also assembled fibers had high specific capacitances of 334 mF cm^{-2} in liquid electrolyte and 218 mF cm^{-2} in solid electrolyte at the current density of 0.1 mA cm^{-2}. [10]

Hu *et al.* (2018) improved the properties of silk fibroin by reinforcing it with graphene oxide. Wet spinning method was used to rectify silk fibroins properties. By the application of reinforcement, the tensile strength increased to as high as 58.7%, and tensile strength increased from 439 to 697 MPa after adding 0.3 wt% FGO nanosheets in FGO/RSF composite fibers with wet spinning. [11]

2.2.3 Solution dry spinning

Difference between solution dry spinning and solution wet spinning is state of solution. Polymers for dry spinning must be soluble in a volatile solvent such as ether or acetone. In this case, polymer solution is heated before being extruded into a hot stream of gas, which is also continuously heated during its passage. Evaporation is occurred during fiber formation. [1] Acrylics, cellulose acetate and triacetate, polybenzimidazole (PBI), spandex and polyvinyl chloride (PVC) can be produced as fiber-shaped by this method. [12]

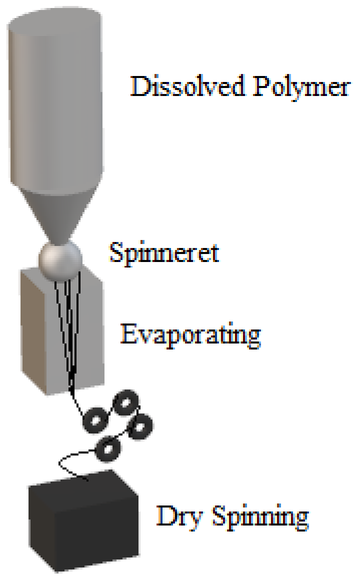

Figure 2.4 : Dry spinning

Zhang *et al.* (2014) achieved to produce lignin-based carbon fiber that have carbon fibers with a tensile strength exceeding most values reported in prior studies by dry spinning method. As a result of this study, carbon fibers with ~7 µm diameter showed a tensile modulus, strength, and strain-to-failure values of 52 ± 2 GPa, 1.04 ± 0.10 GPa, and 2.0 ± 0.2%, respectively. Besides, according to their study, it was produced fibers which had 35% larger surface area as compared with equivalent circular fibers that are typically obtained by melt-spinning. [13]

In a study conducted by Gou *et al.* (2004), predictions of the dynamics of dry-spinning polymer fibers by some two-dimensional modellings in terms of temperature, composition and associated stress profiles. It is valuable data to understand fiber's behaviors before it is produced. [14]

2.2.4 Dry-jet wet spinning

Dry-jet wet spinning method subtype of wet spinning. Addition of wet spinning, this method has a specific dry-jet part before coagulation bath. Name of this method comes from this special part. Dry-jet wet spinning method allows stress relaxation for polymer chains in the air gap. By this way, it can be produced fibers with higher tenacity. [1]

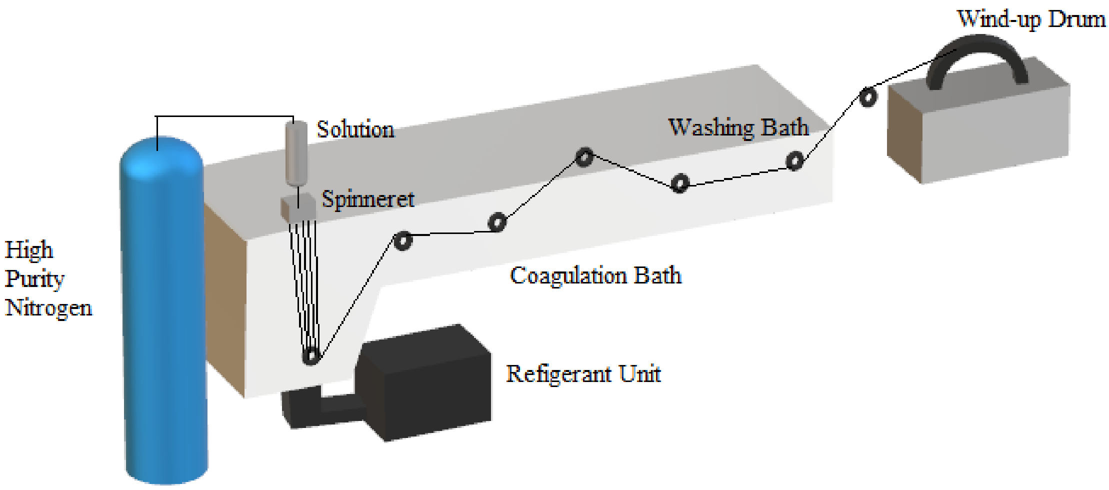

Figure 2.5 : Dry jet wet spinning

Park *et al.* (2001) investigated chemical imidization of aromatic polyamic fiber using dry-jet wet spinning. As a result of this study, they produced samples which had the ultimate stress and initial modulus of the polyamic acid fiber around 268 MPa and 4.1 GPa, respectively. [15]

In the study of Kim *et al.* (2002), it is examined that the double crystallization behavior of dry-jet wet spinning of cellulose/N-methylmorpholine-N-oxide hydrate solutions. It is reported that cellulose/N-methylmorpholine-N-oxide hydrated had great effect on the internal structure and according to their study it was the result of cellulose/N-methylmorpholine-N-oxide hydrates themselves particularly. This is favorable in preparing lyocell fibers with higher mechanical strength. [16]

2.2.5 Gel spinning

High strength polyethylene and aramid fibers can be produced by this method. Gel spinning technology is one of the major production methods for high-strength and high-mechanical-property fibers. In this operation, polymer is not in a true liquid state during extrusion. Due to interchain forces in the resulting fibers, increase of tensile strength can be observed. [1]

Gel spinning can promote the fiber shaped polymer's molecular weight, degree of orientation, crystallinity and fiber density effectively, and that has good effects to increasing the fiber's strength and modulus. Due to its extraordinary properties this method can be used more and more in the near future. [17]

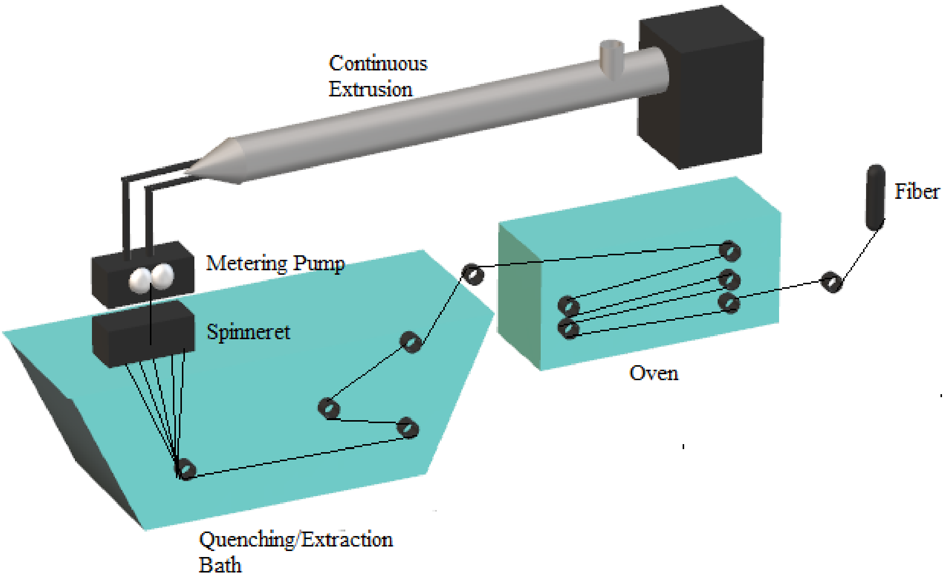

Figure 2.6 : Gel spinning

Tan *et al.* (2011) prepared a study on pregelled gel spinning method and they used it to produce polyacrylonitrile precursor fiber. This method reduced core-shell difference, in addition via gel spinning method fibers have circular cross sections and fewer internal pores. They also examined stress relaxation properties and they observed that by this method fibers had higher elasticity and better developed structure. [18]

Zhang *et al.* (2004) produced polyvinyl alcohol and single wall carbon nanotubes composite fiber by using gel spinning technique. According to their report, the modulus of the produced polyvinyl alcohol/single wall carbon nanotubes composite fiber was 40% higher than that of the control polyvinyl alcohol gel spun fiber.

Crystallinity differences between samples affected the final product properties via gel spinning. [19]

2.2.6 Phase separation spinning

Phase separation spinning involves the extrusion of polymers and solvent in a cooling zone at elevated temperatures. Phase separation usually occurs with the crystallization of the solvent, during the cooling process. The polymers in the extruded filament form fibers during this process, and the solvent can be removed before or after drawing. [1]

2.2.7 Reaction spinning

Prepolymers are used for this method. Prepolymer is extruded into reagent bath and polymerization occurs during spinning. Polyurethane-based elastic fibers can be produced by this method. [1]

2.2.8 Electrospinning

Electrospinning is an electrostatic fiber fabrication technique. The nanoscale fibers are generated by the application of strong electric field on polymer solution or melt. The sub-micron range spun fibers produced by this process, offer various advantages like high surface area to volume ratio, tunable porosity and the ability to manipulate nanofiber composition in order to get desired properties and function. [1]

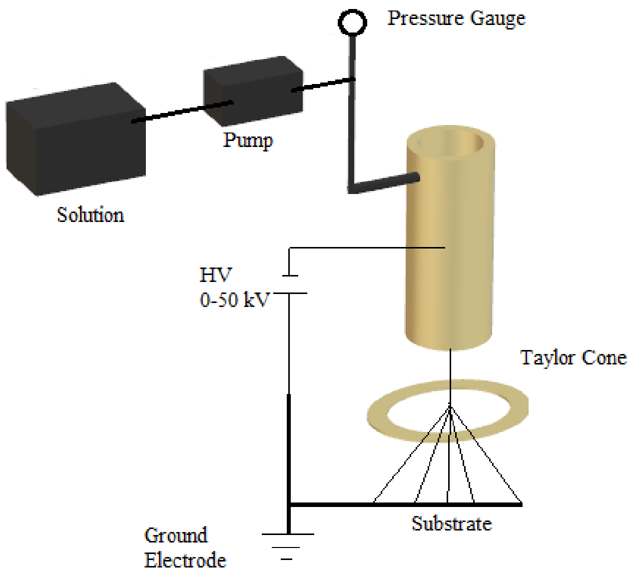

Figure 2.7 : Electrospinning

Basic principles of the system can be listed as below:

- High electrostatic voltage goes through polymer solution

- Liquid is directed to the conical shape which is called Taylor cone
- When voltage reaches the critical value, the electrostatic forces overcomes the solution's surface tension and a stable liquid jet is ejected from the cone tip.
- Solvent evaporates with air and excellent polymeric fiber is obtained. [20]

Nowadays, nanotechnology has become more widespread and as a result of this electrospinning has took an attention by many researchers due to its potential to use for nanotechnological applications. Electrospinning can be used in many areas such as; in filtration, as biosensors, protective clothing applications, energy generation applications, in immobilization of enzymes, as affinity membrane, in cosmetics. [21]
Wei *et al.* (2018) prepared titanium nitride/carbon nanofibers via electrospinning and thermal nitridation process. This study was the first study that microwave absorption performance was investigated based on the polarization loss and impedance matching characteristic. As a result of this study, it is reported that titanium nitride/carbon nanofibers was suitable for lightweight and high-performance microwave absorbing materials. [22]
Dinçer *et al.* (2018) produced activated carbon nanofiber via electrospinning and they investigated optical properties of this material in terms of refractive index, extinction coefficient and dielectric constants. According to the study, activated carbon nanofibers layer allow argument for the applicability of activated carbon nanofibers layer in the area of optoelectronic devices and photon energy applications. [23]
In the present research, Chinnappan *et al.* (2018) examined fabrication of multiwalled carbon nanotubes composites via electrospinning method and also, they investigated the effect of the heat treatment on the mechanical, thermal, and electrical properties of the electrospun fibers. Consequently, they reported that in order to get better properties carbonization at 800 ^{o}C promoted maximum benefits. [24]

2.3 General Properties of Graphene

Graphene is a carbon-based material that has a honeycomb lattice. It has 2D structure and because of this basic structure graphene has extraordinary properties. Based on its unique packing, it gains electron mobility, thermal conductivity, elasticity and stiffness. Since its discovery in 2004, this material has been used by many researchers in many areas like energy storage/generation, electronic devices, sensors etc. As well as its fascinating properties, it can be produced from natural graphite with relatively low cost for large scale. [25,26]

Among other carbon-based materials, graphene fiber has appropriate characteristics for various uses. For instance, because of mechanical flexibility of graphene, it can be used for textile. Also, it has properties like lightweight and ease of functionalization in comparison with conventional carbon fibers.

2.3.1 Electronic properties of graphene

Due to the possibility of varying charge carriers from holes to electrons, graphene has a potential to use in transistors. This property is just applicable for single layered graphene sheets. But dependence is getting weaker if the number of layers increase. It is observed that electron mobility is temperature dependent. [27]

In their innovative study, Novoselov *et al*. (2004) first reported high electrical mobility of single-layer graphene which is ~10,000 $cm^2\ V^{-1}\ s^{-1}$ at room temperature. First graphene-based transistor is obtained by mechanical exfoliation using scotch tape. According to their study, the device showed an ambipolar electric field effect and a high carrier concentration which is $10^{13}\ cm^{-2}$. [26]

Han *et al*. (2017) reviewed progress of graphene-based flexible electronics including light-emitting diodes, solar cells, and field-effect transistors. According to the study graphene has been used in flexible electronic devices, but for practical applications, there are some challenges. Pristine graphene has no band gap; therefore, it is not applicable for field-effect transistors. To overcome the challenges, developments have been accomplished by many researchers and day by day graphene-based materials can be used for electronic devices more commonly. [28]

2.3.2 Mechanical properties of graphene

Carbon-based materials have superior mechanical properties due to cohesion forcer internally. Graphene is also type of carbon-based material and it has also extraordinary mechanical properties. Lee *et al*. (2008) reported that they measured elastic properties and intrinsic breaking strength of free-standing monolayer graphene membranes by nanoindentation in an atomic force microscope. According to their study, tensile strength is determined as 130 GPa, and breaking strength of material is higher than 200 times that of steel, moreover Young’s modulus TPa. [29]

Dikin *et al*. (2007) published that graphene oxide paper has elastic modulus around 32 GPa and fracture strength is around 120 MPa. [30] Due to good mechanical properties, graphene takes a chance to use in several applications.

2.3.3 Thermal properties of graphene

The intrinsic thermal conductivity of graphene is about 2000-6000 $Wm^{-1} K^{-1}$ at room temperature. These values are dependent on defect of surfaces. [27] The possibility of producing a graphene in good quality increases the thermal conductivity of the graphene.

Chu *et al*. (2018) reported that the composites with 30 vol% graphene nanosheets delivered a high in-plane thermal conductivity of 458 W/mK and a low through-plane coefficient of thermal expansion of 6.2 ppm/K, corresponding to a 35% thermal conductivity enhancement and a 64% coefficient of thermal expansion reduction compared to pure cupper, respectively. [31]

Wang *et al*. (2017) produced three kinds of graphene papers with three different thickness graphene nanoplatelets via vacuum filtration method. As a result of this study, they reported thermal conductivity of samples systematically. The in-plane thermal conductivity of graphene nanoplatelets which have thickness of approximately 7 nm achieves 149.2 $Wm^{-1}K^{-1}$, is about 7 times compared to that graphene nanoplatelets which have thickness of approximately 3 nm and graphene nanoplatelets which have thickness of approximately 5 nm. According to their study, it was observed that thermal conductivity of graphene film increased with increasing the thickness of graphene nanoplatelets. [32]

2.3.4 Fabrication of graphene

Producing large scale graphene is one of the biggest challenge in this area. Despite having excellent properties, graphene usage is limited because of lack of appropriate large-scale fabrication method. In this section, some main methods briefly summarized.

2.3.4.1 Micromechanical cleavage

Micromechanical cleavage is well-known process for crystallography and it is one of the most popular method for graphene production. The micromechanical cleavage method is simple method that does not require any special equipment except adhesive tape. [26]

By peeling of the adhesive tape from surface of graphite, graphene flakes can be obtained. Repeating of this simple process is needed to get few-layered or single-layered graphene sheets. [27]

Despite process simplicity, micromechanical cleavage method has limitations due to scalability. For laboratory scale, this method is still easy-to-use, and it is possible to get defect-free graphene.

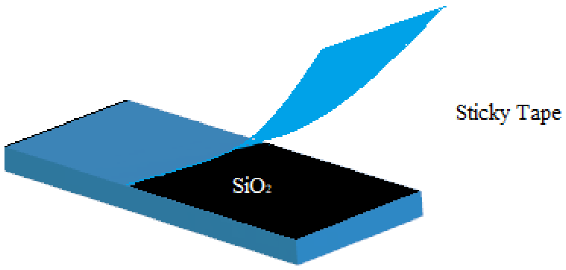

Figure 2.8 : Micromechanical cleavage

Advantages;

- High quality flakes
- Simple preparation method
- Low-cost and easy
- No special equipment needed

Disadvantages;

- Low yield
- Labor intensive (not scalable)
- Uneven films
- Dimensions dependent on initial crystal size

2.3.4.2 Liquid-phase exfoliation

In this technique, weak Van der Waals forces are overcome by ultrasonication or shear forces in liquid-media. Some solvents which are N-methylpyrrolidone and N,N-dimethylformamide commonly used for exfoliation process. [27] The main challenges in exfoliation of graphite in solvents, i.e. suitable solvents with a surface energy around 40 mN m^{-1} is that most of these solvents are not only expensive and corrosive but have also high boiling point and normally toxic.

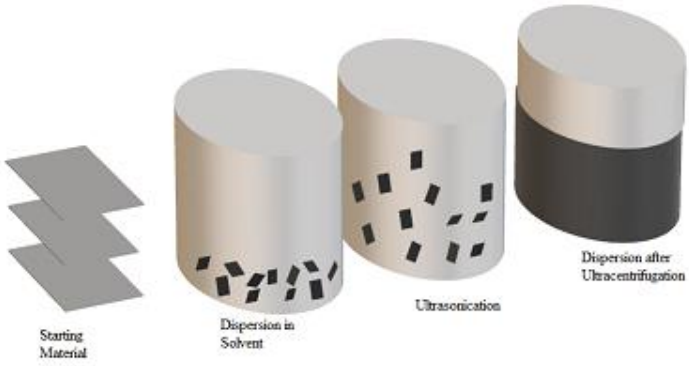

Figure 2.9 : Liquid-phase exfoliation

Advantages;

- High Quality
- Good Scalability
- Low Temperature
- Relatively inexpensive

Disadvantages;

- Small area graphene flakes (<5 µm)
- Low yield of thin graphene layers
- Limited dispersibility
- Limited processability

2.3.4.3 Reduction of graphene oxide

Graphene is also produced by reduction of graphene oxide. Reduction can take places by intercalation of graphite with an oxidant, which introduces functional oxygen groups on the surface of graphene sheets. Due to the functional groups in its structure, graphene oxide can disperse in water. Hummer's method is used to convert graphite oxide to graphene. [27] This method will be explained in next sections.

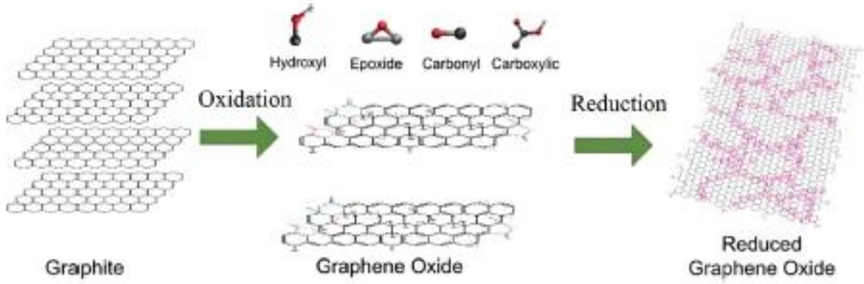

Figure 2.10 : Reduction of GO [27]

Advantages;

- High dispersibility
- Scalable method
- High processability
- High yield
- Relatively inexpensive

Disadvantages;

- Poor electrical/electronic properties
- Fragile stability of the colloidal dispersion
- Potentially explosive process
- Time consuming

2.4 Graphene Oxide and Graphene Oxide Fiber

Graphene is the single carbon layer of graphite. It has the appearance of a 2-dimensional (2D) honeycomb structure and has sp^2- bonded carbon atoms in its structure. [33] It can be directly obtained from graphite or may be obtained from reduction of graphene oxide. Graphene oxide is obtained by the oxidation of graphite by different methods such as Brodie, Hummers or Staudenmaier. Among these, the most common method is Hummers. [34] The exfoliated GO sheets are highly oxidized and featured with the residual epoxides, hydroxides and carboxylic acid groups on their surfaces [35].

With the discovery of the graphene, because of carbon fiber's outstanding performances, this unusual carbon-based material has also been explored for fiber production. As the properties of the GO fibers can be adjusted with various operations, it provides a wide working space for researchers. Generally, graphene fibers are produced by spinning or hydrothermal method [36]. Among spinning methods wet spinning method is very suitable for graphene oxide fiber production.

First studies on graphene fiber production starts from the 2011 years [33],

General principle of continuous fiber production consists of three main steps:

1) Oxidation of graphite which is sometimes exfoliated by high temperature heating process,

2) The dispersion in suitable solvents such as water in order to disperse and separate the flakes from each other,

3) The coagulation of GO dispersion in suitable coagulation bath in order to obtain continuous GO fiber.

2.4.1 Applications of graphene oxide fiber

As seen from literatures, since 2010s, there are very limited studies performed on continuous Graphene Oxide (GO) fiber production by wet spinning technique and those studies were mostly focused on reduction method, hollow fiber production, composite fiber production, potential applications in catalysts, sensors, etc.

In their study, Cong *et al*. (2012) reported an approach to produce graphene fibers by processing GO solutions via wet-spinning technique followed with chemical reduction. Firstly, they used and clarified mechanism of GO fibers with coagulation bath of hexadecyl trimethyl ammonium bromide solution with a low concentration. At the end, they produced fibers that has mechanical strength approximately 182 MPa and high electronic conductivity as approximately 35 S/cm. [37]

Chen *et al*. (2017) investigated mechanical behaviors of GO fiber-cement composites. According to study that was carried by Chen *et al*. GO carbon fiber cement composite with adding 0.06% GO and 1% carbon-fiber was increased by 23.89%, whereas the increment of the flexural tensile strength of the composite was increased by 138.44%. These results are valuable for civil and transportation structures. [38]

Mazzoli *et al*. (2018) examined electromagnetic shielding properties of graphene oxide powder and metallic fibers. From experimental results, it can be observed that cementitious composites with addition of GO microparticles and steel fibers can be considered a promising new class of EM shielding materials. The use of steel fibers alone or combined with GO microparticles produced the better results in terms of mechanical properties and EMI shielding effectiveness of the cementitious composites. [39]

Terasawa *et al*. (2017) compared electrochemical and electromechanical properties of poly(vinylidene fluoride-co-hexafluoropropylene)-based actuators using graphene oxide (GO) or graphene (G)/vapor grown carbon fiber (VGCF)/ionic liquid (IL) composite gel electrodes formed are compared with those of actuators using only GO, only G, and only SWCNT. Based on data they had achieved at the end of study, graphene combined with VGCFs exhibit promise as energy-conversion devices and wearable electrode materials. [40]

Meng *et al*. (2016) reported electromechanical response of chemically reduced graphene oxide fiber. According to their study, they determined rGO fiber's tensile strength (159 MPa) and electrical conductivity (170 S/cm). Reduction of graphene oxide gives fibers unique properties. This novel electromechanical actuation makes rGO fibers promising to serve as new actuators and sensors. [41]

Ucar *et al*. (2016) investigated the effect of nozzle size, feed rate, and Vitamin C reduction time on graphene fiber properties and found that improved electrical conductivity and mechanical performance can be obtained by varying feed rate and reduction time. [42]

Huang *et al.* (2013) varied the wet spinning parameters of graphene oxide hydrogel to obtain graphene fibers and ribbons and concluded that better electrical properties in along with higher elasticity and elastic recovery was obtained with graphene ribbons compared to graphene fibers. [43]

Yongqiang He *et al*. (2012) had prepared alginate/graphene oxide fiber by wet spinning method and observed that by the incorporation of GO significantly improved the strength of the NaAlg/GO fibers. [44]

Wujun Ma *et al*. (2016) had manufactured MnO_2 nanowire/graphene hybrid fibers to improve electrochemical properties for supercapacitor applications. The electric double-layer capacitance of graphene was observed to improve which was thought to be due to effect between MnO_2 nanowires and graphene. [45]

Zhang *et al*. (2018) fabricated human motion monitoring system for professional athletes by using graphene coated fiber sensor. The recorded data indicated ultrahigh sensitivity and it has very large sensitivity range. Stretching, torsion and bending tests had been performed and motion monitoring system was examined in their study. Results were shown that wearable graphene-coated fiber sensors which has been fabricated in a low-cost and very easy way can not only be successfully used in human motion monitoring in sports but also have very broad application prospects in the field of monitoring human health. [46]

Li *et al*. (2018) prepared graphene oxide-chitosan composite fibers by wet spinning method and they examined mechanical behavior of composite fibers. It is shown that introduction of graphene oxide at 4 wt% loading improves tensile strength of chitosan fiber. Tensile strength of samples reached 165.8 MPa where pure chitosan fiber has tensile strength of 96.7 MPa. They also carried thermodynamic investigations to determine adsorption properties of sample that they produced. It was observed that the adsorption reaction is a spontaneous and exothermal process. [47]

Gao *et al*. (2015) demonstrated a novel humidity sensor based on power leakage at resonance wavelength in a reduced graphene oxide coated hollow core fiber. According to experimental results the sensitivity of up to o 0.22 dB/% RH is achieved. rGO coated hollow core fiber humidity sensor has potential for use of sensor applications. [48]

In their study, Xiong *et al*. (2015) fabricated reduced graphene oxide-carbon nanotubes (CNT) grown on carbon fiber by a combination of electrophoretic deposition (EPD) and chemical vapor deposition. They measured electrochemical properties of their samples and it displayed a higher specific capacitance of 203 F g^{-1}, 4 times higher than that of pure carbon fiber. This result shows that prepared hybrid material is candidate for flexible supercapacitor applications. [49]

To obtain GO fiber, the reduction processes can also be varied and have been studied in the literature. Hydrazine was used as a reducing agent by Jalili *et al*. (2013) and they observed an increase on electrical conductivity of graphene fiber; however, a loss in mechanical properties were observed which was thought to be because of expansion of GO fiber diameter after hydrazine treatment. [50]

3. EXPERIMENTAL PROCEDURE

3.1 Materials

Expandable graphene-GIC with a thickness of 30 μm, diameter of 300 μm is supplied from Grafen Chemical Industries (Grafen Co). $KMnO_4$ (Merck, M: 158.03 g/mol), H_2SO_4 (Merck, M: 98.08 g/mol), and HCl (37%, Merck) are supplied from Merck, and $NaNO_3$ (ZAG, 7631-99-4, M: 84.99 g/mol) from Zag Ltd., activated carbon nanoparticles from Grafen Chemical Industries Co, (average particle dimension <100 nm, spherical, purity>95%). Distillated water and argon gas were used for the sample preparation and testing steps.

3.2 Methods

3.2.1 Thermal exfoliation

Fixed-bed tube oven was used for exfoliation of expandable graphite. During exfoliation, argon gas which is inert was fed at 0.5 standard liter per minute.

Figure 3.1 : Fixed-bed tube oven

This process involves extraction of individual graphene layers by overcoming the Van der Waals forces between the adjacent layers which enhances the surface area and efficiency of the oxidation process. Quartz tube which has two parts is used for the exfoliation. One part of the tube has fish tail part and the other part is closed.

Figure 3.2 : Relatively fish tail part and lid part of quartz tube

First, tube was fixed and at the fish tail part argon was fed into the tube. Sample which would be exfoliated was put into the tube at the other side and lid was closed. Different exfoliation temperatures and periods were applied to the samples and listed at Table 3.1. Afterward, due to control the media, argon gas fed into the tube at 0.5 standard liter per minute for 10 minutes and feeding rate of argon gas were decreased to 0.2 standard liter per minute. At the end of all these steps, exfoliated sample were taken into the tube and packaged carefully to protect it.

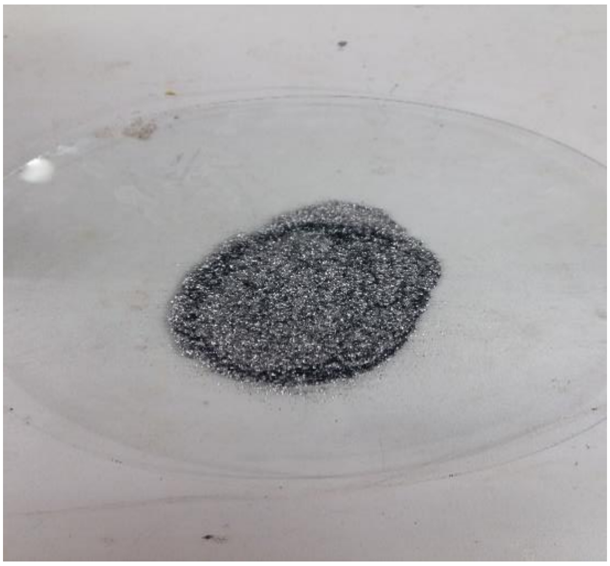

Figure 3.3 : Graphene, before exfoliation step

Figure 3.4 : Graphene, after exfoliation step

3.2.2 Preparation of graphene oxide dispersion by modified Hummers method

After the exfoliation step, modified Hummers method was used to obtain GO dispersion from exfolidated graphite flakes. [51]

- $KMnO_4$:H_2SO_4=1:20 (mass)
- Graphene:H2SO4=1:100 (mass)
- Graphene:NaNO3=1:0.5 (mass)

According to listed mass rates, for 1 gram of expandable graphene 0.5 gram $NaNO_3$ were used. Natural graphite flakes, $NaNO_3$ and 100 ml H_2SO_4 were mixed together and for 5–10 min, this mixture was uniformly dispersed with a magnetic stirrer in an ice bath at 0^{o}C, followed by gradual addition of 5 g $KMnO_4$ to the mixture. First, mixture had been stirred for 2 hours in the ice bath after that step, it had been stirred for 2 hours more at 35 ^{o}C without ice bath. At the end of the stirring steps, mixture was diluted with 220 ml distilated water, then temperature was increased to 98 ^{o}C carefully and mixture was diluted again with 770 ml water. (Figure 3.5)

Figure 3.5 : Mixture, before the addition of hydrogen peroxide

Subsequently, before treatment of 6 ml hydrogen peroxide (H_2O_2) to terminate the reaction the mixture was kept in distilled water for five days, while the solution turned into yellow color. (Figure 3.6)

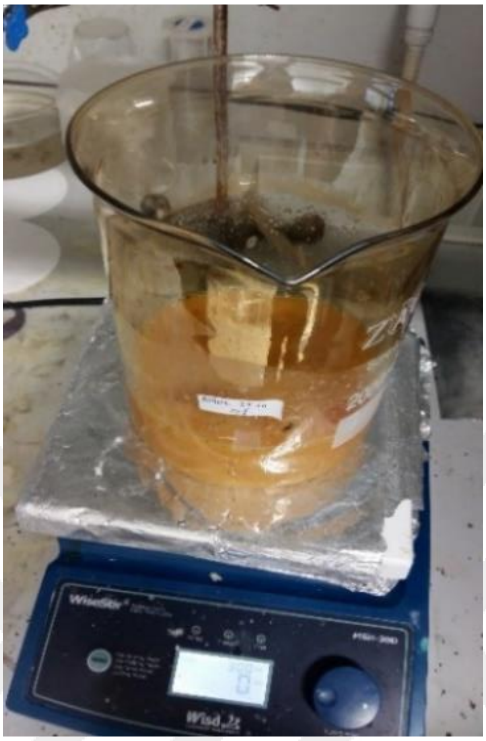

Figure 3.6 : Mixture, after the addition of hydrogen peroxide

Then the mixture was centrifuged in centrifuge tubes. In a centrifuge (Nüve, NF800R) running at 5500 rpm, 1 M HCl was used for washing three times. Then GO dispersion was centrifuged with distilled water until the pH of the solution reached about 5–6. The concentration of mixture was fixed at 20 mg/ml.

3.2.3 Mechanical homogenization and ultrasonication

The prepared graphene oxide solutions were dispersed at 10,000 rpm for 90 min with a mechanical homogenizer (WiseTis Homogenizer, HG-15D). In addition, prior to mixing with a mechanical homogenizer, in order to examine the effect of ultrasonic waves onto the homogenization, a sample solution was dispersed with an ultrasonic homogenizer (Bandelin Electronic) for a short time and a long time, i.e. 15 and 60 min. Following the ultrasonic homogenization step, the sample solution was mixed with a mechanical homogenizer at 10,000 rpm for 90 min.

Different exfoliation time and temperatures were used to compare properties of fibers and also additional applications like adding AC were utilized relatively. According to specifications samples were coded and listed on Table 3.1.

Table 3.1 : Sample codes

Types	Operations
1050C-35s	Thermal exfoliation at 1050 ^oC for 35 second
1020C-35s	Thermal exfoliation at 1020 ^oC for 35 second
1020C-45s	Thermal exfoliation at 1020 ^oC for 45 second
1000C-15s	Thermal exfoliation at 1000 ^oC for 15 second
1000C-35s	Thermal exfoliation at 1000 ^oC for 35 second
1000C-35s-Ult-S	Thermal exfoliation at 1000 ^oC for 35 second and ultrahomogenisation were performed for 15 seconds
1000C-35s-Ult-L	Thermal exfoliation at 1000 ^oC for 35 second and ultrahomogenisation were performed for 60 seconds
1020C-35s-AC	Thermal exfoliation at 1020 ^oC for 35 second and AC was added

3.2.4 Wet spinning of graphene oxide

Reapectively, the prepared dispersion was injected into coagulation baths at a feed rate of 20 ml/h, with a needle which had inner diameter as 0.69 mm. Before spinning of graphene oxide, adjustment of mg/ml had been done. Wet spinning technique used for spinning of graphene oxide fibers and theree types of coagulation baths had been used during the process and ingredients of coagulation baths (CB) were listed on the Table 3.2.

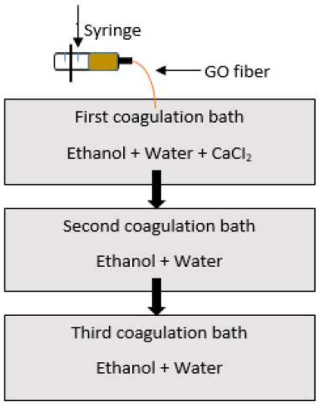

Figure 3.7 : Mixture, before the addition of hydrogen peroxide

Table 3.2 : Coagulation baths

Type	Substances
First CB	30 ml ethanol+70 ml water+ 5 % wt. $CaCl_2$
Second CB	40 ml ethanol+60 ml water
Third CB	50 ml ethanol+50 ml water

3.3 Characterization

3.3.1 Scanning electron microscopy (SEM)

The surface and crosssectional morphologies of the GO fibers were characterized by Scanning Electron Microscopy (QUANTA FEG 200) in ESEM (Environmental SEM) mode. Samples were coated with Au/Pd (Quorum, SC7620) under vacuum conditions (2×10^{-2} mbar) prior to SEM measurements.

3.3.2 Tex number

Determination of tex number is important for characterization of fiber properties. Three different fiber samples were selected and length of these fibers were measured separately. After all these measurements, the weight was calculated for the fiber of 1 km length by precision scale.

3.3.3 Electrical conductivity

For electrical conductivity measurements, the electrical resistance values of the graphene oxide fiber samples, 1 cm in length, were measured with a two probe Microtest 6370 LCR meter. Average value of more than 10 measurements for each GO fiber sample has been taken. Electrical conductivity coefficient was calculated according to the below formulation.

$$\rho = L/(A * R) \tag{3.1}$$

Where; ρ = coefficient of electrical conductivity (S/cm), R = electrical resistance (ohm), A = cross-sectional area of fiber (cm^2), and L = Fiber length between the probes (cm).

3.3.4 Tensile testing

Tensile strength and elongation of the graphene oxide fiber samples were measured using a Usel, UNF 15 Tensile Tester according to the ASTM D3822–07 standard. A gage length of 10 mm and a test speed of 1 mm/min were used. Average value of more than 10 measurements for each GO fiber sample has been taken.

3.3.5 X-ray photoelectron spectroscopy (XPS)

The chemical composition of the GO fiber was analyzed using a Thermo Scientific K-Alpha, X-ray Photoelectron Spectrometer. The binding energies were referenced to the C 1 s line. The XPS spectra were recorded using k-alpha radiation. The survey scan was recorded at a pass energy of 150 eV and an energy step size of 0.1 eV s^{-1}. Analysis chamber pressure was about 8×10^{-8} mbar.

3.3.6 Atomic force microscopy (AFM)

The surface roughness of graphene fibers were scanned with an Atomic Force Microscope (Ambios Technology, Santa Cruz, CA). A rectangular, NSC15 series, silicon tip (with a radius < 10 nm, a frequency of 325 kHz and a force constant of 40 N/m) was used as a probe to scan the surface in a non-contact mode, at room temperature.

3.3.7 X-ray diffraction (XRD)

The XRD patterns of samples were obtained using a X-ray diffractometer (Bruker D8 Advance) with Cu Kα radiation (λ = 1.54056 Å) under a voltage of 40 kv and a current of 200 mA. The diffraction patterns were firstly peak differentiated and fitted by Diffracplus EvaTM 3.0 to obtain the peak position and full-wide at half maximum (FWHM). Using a TOPASTM 4.0 software, the interlayer distance and crystal size were calculated according to the Bragg and Scherrer formula, crystal size divided by interlayer distance represents the number of layer.

4. RESULTS AND DISCUSSION

4.1 Scanning Electron Microscopy (SEM)

The surface and crosssectional morphologies of the GO fibers were characterized separately and they are demonstrated as cross sectional (CS) (20000x) and longitudinal (L) (1000x), respectively.

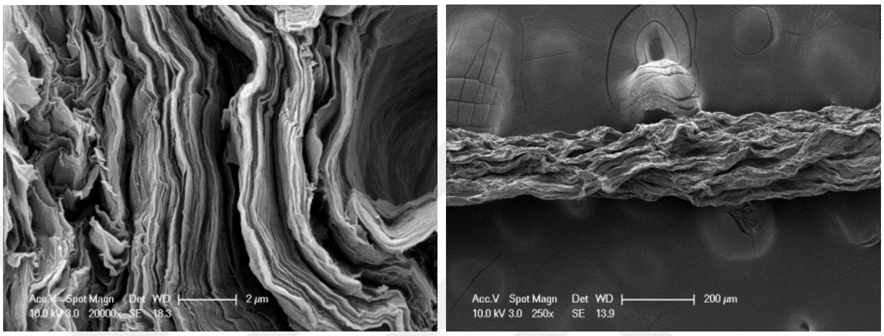

Figure 4.1 : SEM micrographs of 1050C-35s referenced sample, CS, L

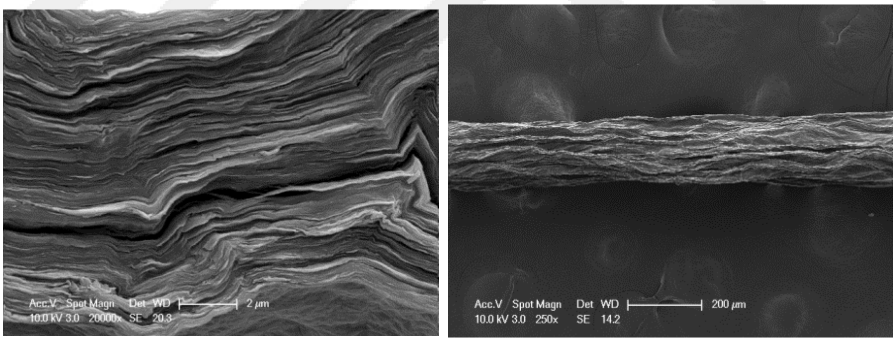

Figure 4.2 : SEM micrographs of 1020C-45s referenced sample, CS, L

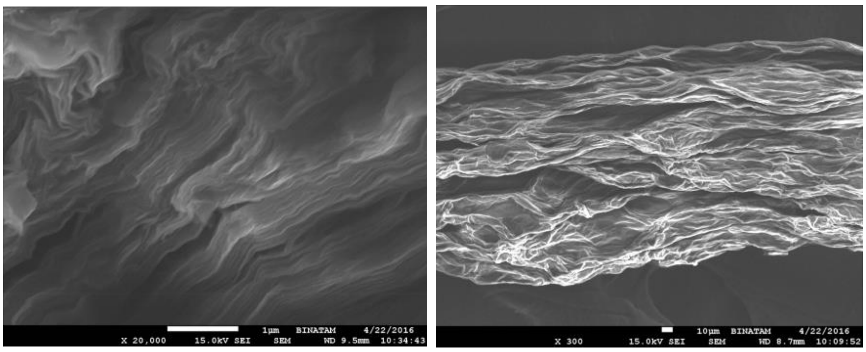

Figure 4.3 : SEM micrographs of 1000C-15s referenced sample, CS, L

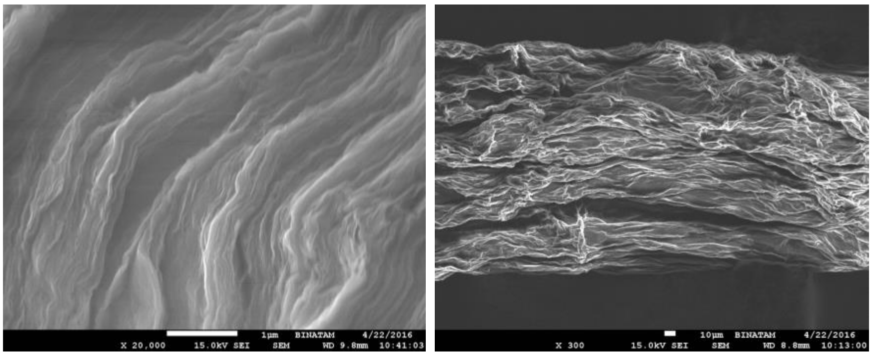

Figure 4.4 : SEM micrographs of 1000C-35s referenced sample, CS, L

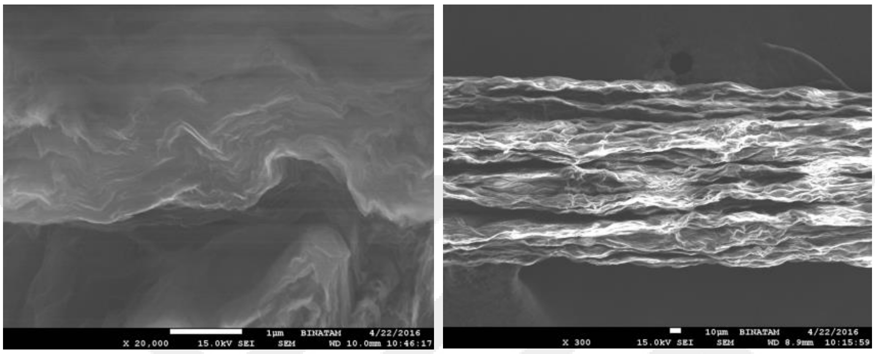

Figure 4.5 : SEM micrographs of 1000C-35s-Ult-S referenced sample, CS, L

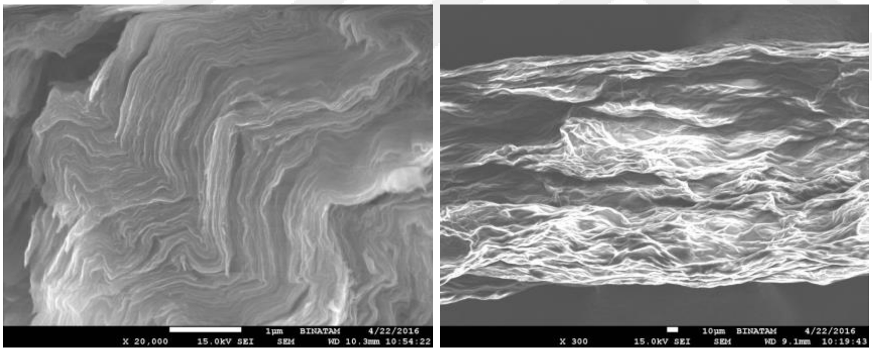

Figure 4.6 : SEM micrographs of 1000C-35s-Ult-L referenced sample, CS, L

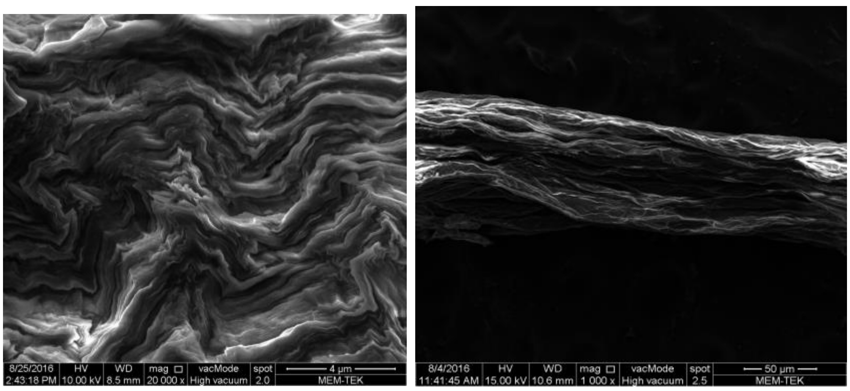

Figure 4.7 : SEM micrographs of 1020C-35s referenced sample, CS, L

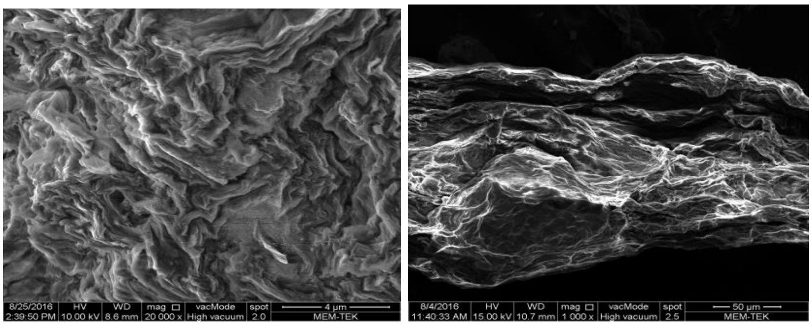

Figure 4.8 : SEM micrographs of 1020C-35s-AC referenced sample, CS, L

As seen from Figure 4.2, appearance of sample with 1020C-45s is nonporous and more ordinary structure than sample with 1020C-35s and 1020C-35s-AC. This situation can be result of more exfoliation and separation of GO flakes from each other or less and slowly coagulation during spinning. Gratingly and nonsmooth CS images have been taken for the sample with 1020C-35s-AC because of AC. When the literature is searched, it is also known that heating above 1000°C causes rapid degeneration, which causes voids and defects in the surface and fluctuations. This situation is confirmed by the increase in peak-valley Rpv for 1050C-35s with small decreasing of Ra value that is relatively close and almost the same. As we can see on the figures that 1000C-35s-Ult-L is a little more compact compared to 1000C-35s-Ult-S and 1000C-35s, which is confirmed by the drop of peak-valley Rpv and Ra (average height) in AFM for 1000C-35s-Ult-L. The size of the particles contained in the samples subjected to ultrasonication for a long time showed a decrease with the effect of the generated sonic force. It is known that as the particle size on the surface decreases, the roughness of the surface also decreases [54] This is why the Rpv value is low.

4.2 Tex Number

Results (Table 4.1) show that because of the ultrasonicaton time, some chemical bondings are broken and this situation causes decreasing of molecular weight. Therefore, lower weight and lower tex numbers are obtained. [55,56,57,58] 1000C-35s has a higher Tex value than 1000C-15s, the increase in exfoliation can be explained by an increase in the crystallite size and a decrease in the interlayer spacing. In addition, according to the XPS analysis, the C/O value is slightly lower at 35s, suggesting that more oxygenated function groups may be attached, all of which may have led to an increase in Tex [59,60] 1050C-35s has higher tex value than 1000C-35s. It is a fact that is known to increase degradation by rapid exfoliation at very high temperature [52,53]. This may result in less functional group binding and less Tex at 1050°C. XPS results also indicate that there are functional groups with less oxygen at 1050 °C with higher C/O ratio. Addition of activated carbon particles causes slight increase of tex value.

Table 4.1 : Tex numbers

Samples	Tex numbers
1050C-35s	37.66
1020C-35s	13.35
1020C-45s	36.5
1000C-15s	26.66
1000C-35s	42.77
1000C-35s-Ult-S	25.80
1000C-35s-Ult-L	17.03
1020C-35s-AC	14.47

4.3 Electrical Conductivity

Electrical conductivity is important parameter to determine characteristics of GO fibers. Several researches have been done to improve electrical properties of carbon based materials. GO fibers have advantage due to functional groups which are located into the GO flakes. Many parameters can affect electrical conductivity. These were also examined in this study and it was seen that C/O ratio, morphological properties and electrical networks had vital effect on condutivity properties. Table 4.2 represents that the long ultrasonication at reference 1000C-35s-Ult-L or short ultrasonication at 1000C-35s-Ult-S do not have a significant effect on the electrical conductivity, but the conductivity is slightly higher than reference 1000C-35s. The C/O ratio in the short ultrasonication is not very high, even in the lowest, but the dispersion of the particles with an ultrasonication at an optimum value can provide an explanation that the long ultrasonication has a very high C/O. Smaller flakes can be played an important role in this situation. Flakes filled the gaps along the conductivity path and gave the sample better conductivity properties. The homogenous distribution may have increased [61,62,63], which may have caused the continuity and density of the contact points and the increase in the conductivity value. When we look at the results of samples 1000C-35s and 1050C-35s, it can be observed that electrical conductivity values is not effected by an increase in exfoliation temperature. As we can see on the SEM images, for sample 1050C-35s, rough and porous structure were obtained due to the voids which occurred by temperature. Therefore because of void formation electrical conductivity got worse accordingly. Furthermore, addition of AC did not affect electrical conductivity significantly. When it was compared with sample referenced 1020C-35s, it can be seen that there was not any improve in electrical conductivity properties. Because of this situation, there was no meaning of adding this step to the process in terms of electrical conductivity.

Table 4.2 : Electrical conductivity

Samples	Average conductivity (S/cm)	Standard deviation	Coefficient of variation (CV%)
1050C-35s	$8.60*10^{-4}$	$1.28*10^{-4}$	14.9
1020C-35s	$2.35*10^{-3}$	$4.94*10^{-4}$	21
1020C-45s	$3.83*10^{-4}$	$8.44*10^{-5}$	22
1000C-15s	$1.19*10^{-3}$	$3.57*10^{-4}$	29.9
1000C-35s	$7.33*10^{-4}$	$1.72*10^{-4}$	23.4
1000C-35s-Ult-S	$1.09*10^{-3}$	$2.44*10^{-4}$	22.4
1000C-35s-Ult-L	$1.23*10^{-3}$	$3.70*10^{-4}$	30
1020C-35s-AC	$1.05*10^{-3}$	$3.03*10^{-4}$	28.9

4.4 Tensile Testing

The mechanical properties of sample with 1020C-35s (Table 4.3) are better than sample with 1020C-45s. This situation can be result of strong bonding between layers due to functional groups which can be seen also in XPS results. The massive decrease in mechanical properties of sample with 1020C-35s-AC is because of AC which causes gratingly and porously structure seen from CS images according to SEM. There is not much difference in strength value between 1000C-15s and 1000C-35s but it is seen that the elongation at break is slightly higher in 1000C-15s application. The roughness values are higher in 1000C-15s application, which can be explained by the fact that the elongation at break is higher due to the higher opening at break at the same time as the accordion. Due to the ultrasonication, 1000C-35s-Ult-S and 1000C-35s-Ult-L have higher strength and elongation than 1000C-35s. There are many factors that affect the mechanical properties. We can see from the literature that one of these is the uniformity of the dispersion and that the dispersion can be optimized by ultrasonically applying it under optimum conditions [64,65] In this respect, short ultrasonication may have a positive effect compared to mechanical dispersion, long ultrasonication may worsen mechanical properties due to the risk of breaking molecular bonds, and other factors such as holding the fibers together may increase the breaking strength. Considering the AFM values, the short ultrasonicated samples have a higher roughness than the long ultrasonicated samples. Although it may aggravate the mechanical properties by breaking and deforming the ultrasonic bonds for a long time, the better dispersion than the mechanical application may have provided the breaking strength to be higher. Therefore, it is also clear that the dispersion state of the flakes, their orientation and the effect of the mechanical properties of the intertwining state are important. Furthermore, it has been found that the 1050C-35s, 1020C-45s, 1020C-35s provide relatively better mechanical properties.

Table 4.3 : Tensile properties

	Breaking strength (MPa)			Breaking elongation (%)		
Samples	Mean	Standard deviation	Coefficient of variation (CV%)	Mean	Standard deviation	Coefficient of variation (CV%)
1050C-35s	29.38	7.89	26.85	6.03	1.75	29.03
1020C-35s	40.50	1,20	27.10	4.10	0.87	26.00
1020C-45s	33.19	9.08	27.36	3.39	0.99	29.39
1000C-15s	9.27	2.57	27.76	8.65	1.61	18.55
1000C-35s	10.17	1.97	19.39	3.88	0.88	22.71
1000C-35s-Ult-S	21.51	3.29	15.3	3.29	0.76	23.15
1000C-35s-Ult-L	19.64	5.09	25.96	2.43	0.64	26.54
1020C-35s-AC	3.90	2.30	25.50	5.70	0.85	24.50

4.5 X-ray Photoelectron Spectroscopy (XPS)

Table 4.4 : Elemental compositions

	Atomic percentages (%)		Peak binding energy (eV)		Atomic ratio
Samples	C	O	C	O	C/O
1050C-35s	77.8	18.9	285.0	532.3	4.1
1020C-35s	68.0	29.1	285.0	532.9	2.32
1020C-45s	74.7	22.1	285.0	532.2	3.38
1000C-15s	83.8	14.9	285.0	532.4	5.6
1000C-35s	74.6	23.8	285.0	532.1	3.2
1000C-35s-Ult-S	79.7	17.8	285.0	532.3	4.5
1000C-35s-Ult-L	71.0	23.7	285.0	532.1	2.9

Table 4.5 : Binding energies and percentages

	Peak 1		Peak 2		Peak 3	
	C—C or C—H		—C—OH or —C—OR		—C=O	
Samples	Binding Energy	%	Binding Energy	%	Binding Energy	%
1000C-15s	284.79	45.31	286.16	7.45	288.33	7.54
1000C-35s	284.78	19.64	286.01	26.33	287.46	14.47
1000C-35s-Ult-S	284.76	27.05	286.23	18.88	288.07	12.22
1000C-35s-Ult-L	285.15	14.21	286.34	25.16	288.15	8.77
1020C-35s	285.02	10.53	285.51	20.78	287.15	50.53
1020C-45s	284.92	16.79	286.21	28.69	288.05	9.2
1050C-35s	284.98	26.78	286.12	20.98	288.06	10.5

When ultrasonication is applied for a long time, the particles in the form of large platters are broken and shrink, which causes the surface area to grow. As a result, free oxygen in the medium may be finding more space to attach. As a result of the exfoliation process performed at 1050°C, the functional group was further reduced compared to 1000°C, resulting in a higher C/O ratio. When a detailed C scan is performed on the samples as an XPS analysis, the graphs are obtained. The blue curves shown in the graphs refer to the whole of the scan, while the curves labeled 1,2 and 3 are separated from the components of this blue curve. According to BE values, this peak separation tells us what kind of bond we have in our material. The numerical and percentage values are shown in Table 4.5.

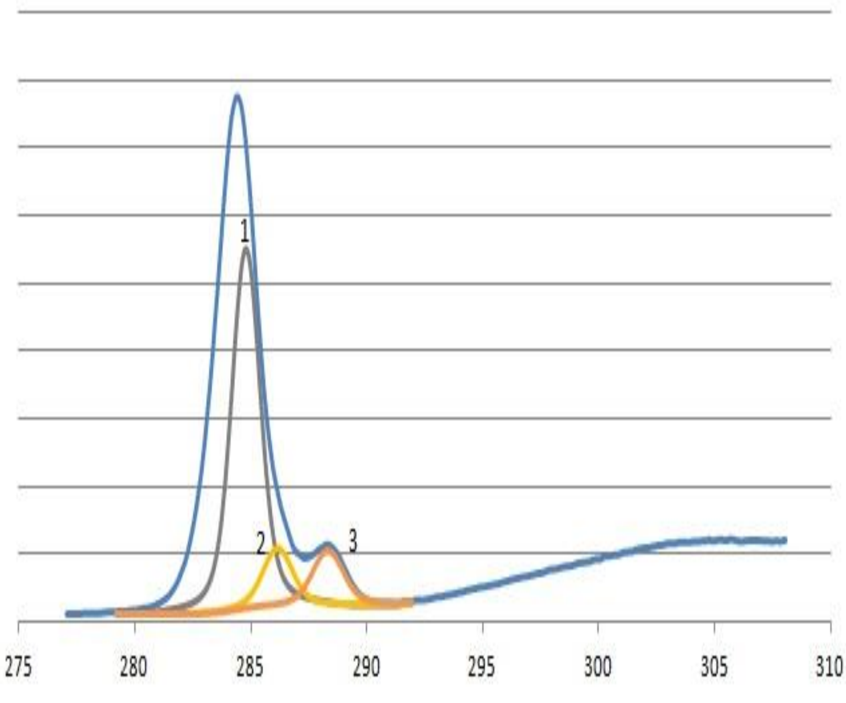

Figure 4.9 : XPS graph of 1000C-15s

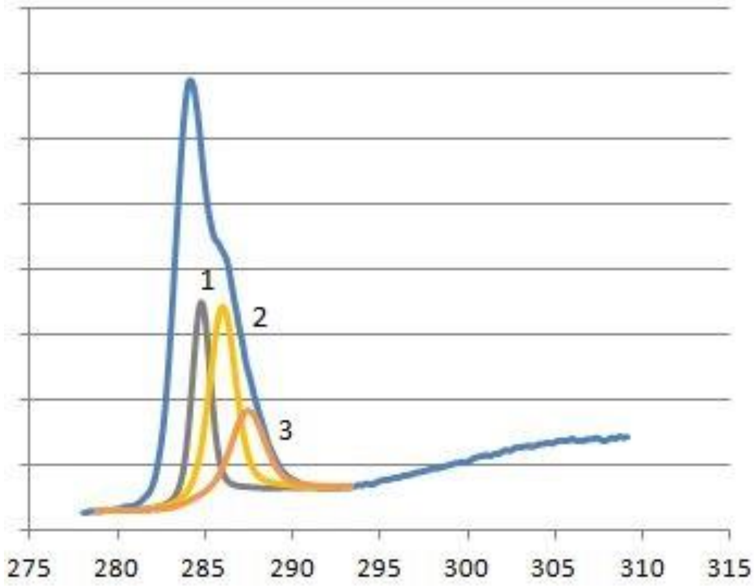

Figure 4.10 : XPS graph of 1000C-35s

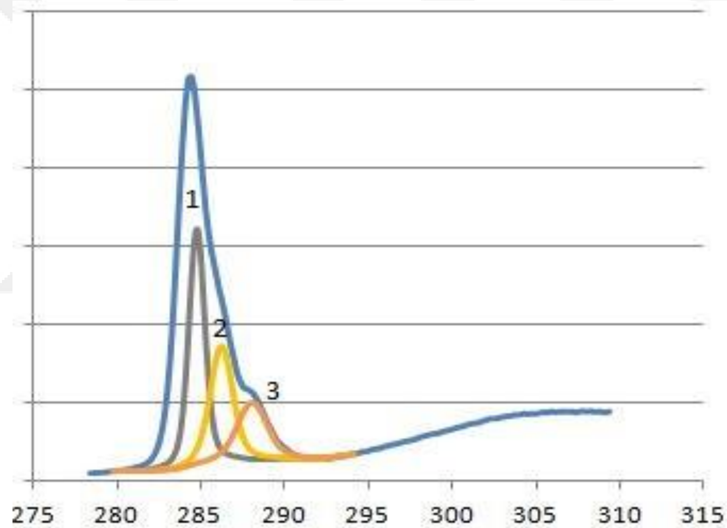

Figure 4.11 : XPS graph of 1000C-35s-Ult-S

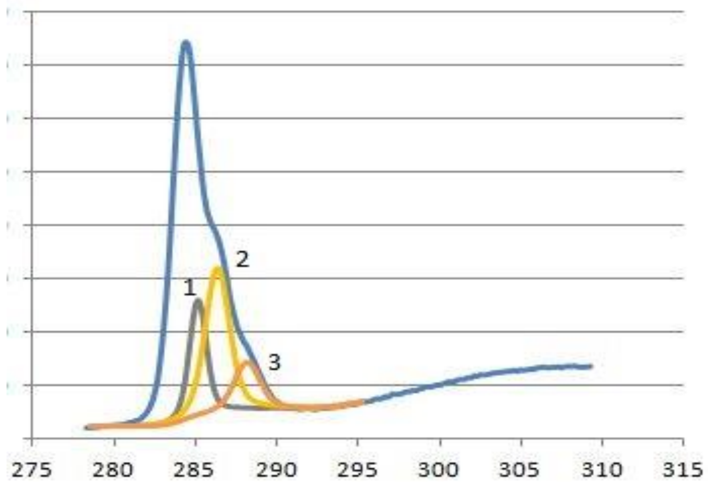

Figure 4.12 : XPS graph of 1000C-35s-Ult-L

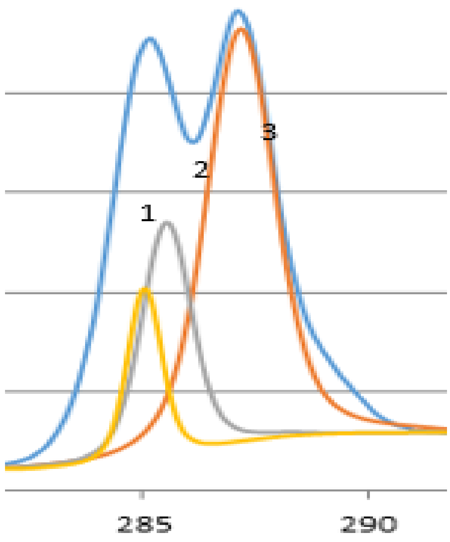

Figure 4.13 : XPS graph of 1020C-35s

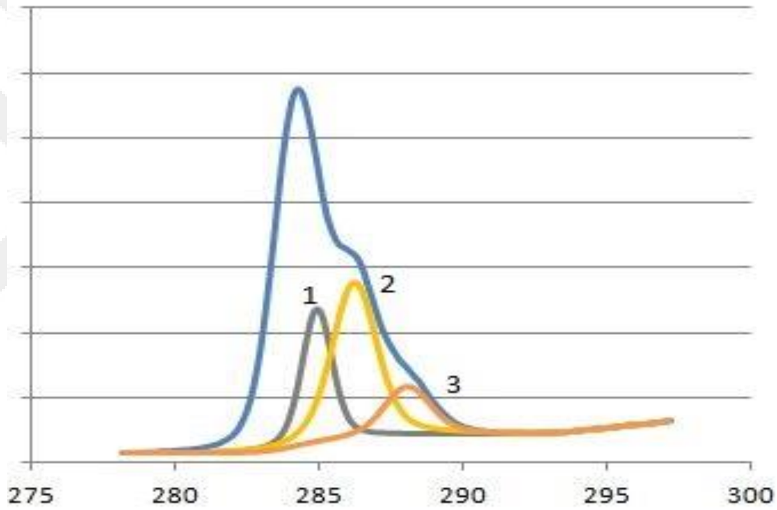

Figure 4.14 : XPS graph of 1020C-45s

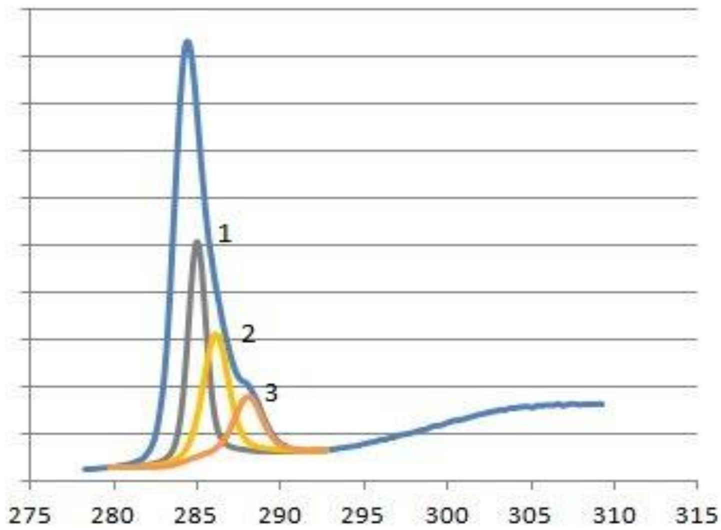

Figure 4.15 : XPS graph of 1050C-35s

4.6 Atomic Force Microscopy (AFM)

Table 4.6 : AFM results of samples

Sample	Avarage height (nm)	Rq (nm)	Ra (nm)	Rpv (nm)
1000C-15s	776.995	222.985	166.910	1404.191
1000C-35s	327.683	133.258	113.270	543.425
1000C-35s-Ult-S	480.021	136.557	112.651	567.555
1000C-35s-Ult-L	272.035	83.543	64.015	395.920
1020C-45s	1286	400	309	2899
1050C-35s	2302	797	683	2755
1020C-35s	4948	829	642	4963

According to AFM values, it is seen that at a temperature of 1000^{o}C, the short-time exfoliation for 15 seconds, is more rough than 35 seconds. Possible reason is that since the opening of the plates in 15 seconds is not too much, massive and very thick plates may cause more indentation in the structure and may cause less homogeneous distribution in the coagulant bath, so that at the moment of coagulation, more separation of massive particulates at the moment of separation of liquid structure in GO dispersion, it is thought that the indentation may also increase. Compared with the exfoliating process applied at 1000^{o}C and 1050^{o}C for 35 seconds, the increase in temperature also increased surface roughness due to formation of large crystal structures. [66,67,68,69] One of the possible reasons for the increased roughness due to the increase of the ultrasonic time is that as the ultrasonic interval increases, the flakes may become smaller and smaller flake particles may cause less rough [53]. At the same time, the ultrasonic short has been found to be slightly higher in roughness than the mechanical application, and it is known that cavities and cavities will develop on the surface with ultrasound [57,58].

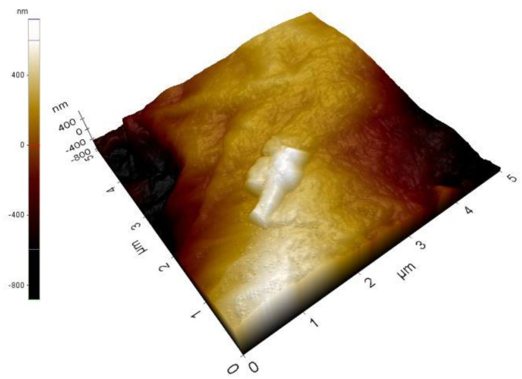

Figure 4.16 : AFM profile of 1000C-15s

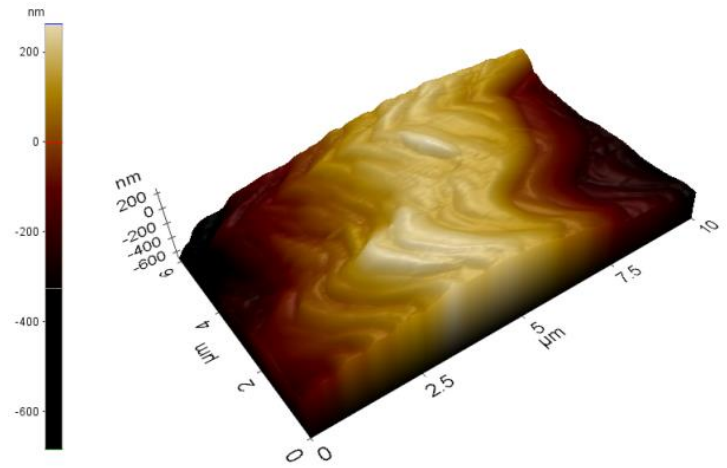

Figure 4.17 : AFM profile of 1000C-35s

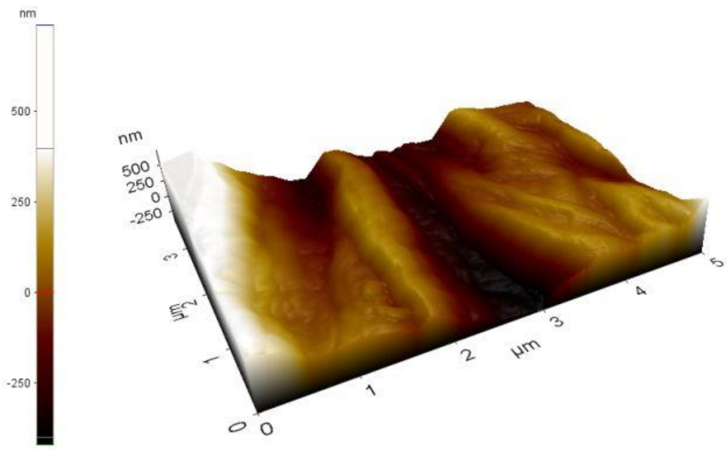

Figure 4.18 : AFM profile of 1000C-35s-Ult-S

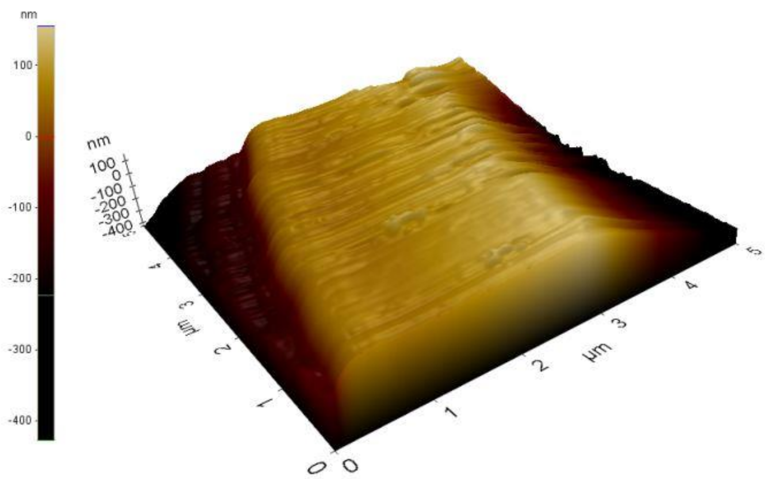

Figure 4.19 : AFM profile of 1000C-35s-Ult-L

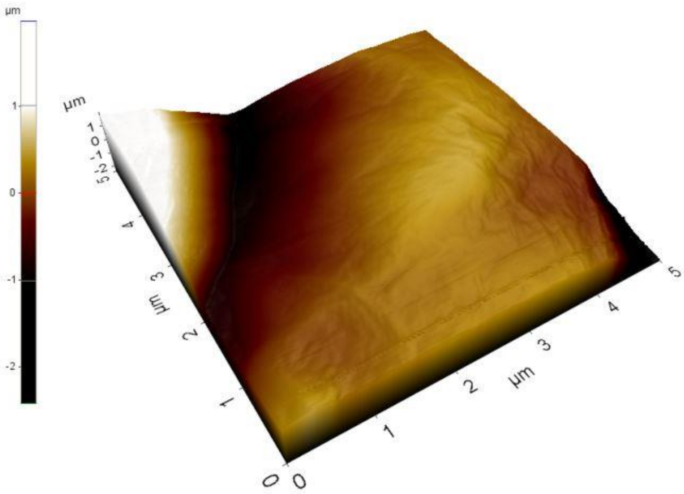

Figure 4.20 : AFM profile of 1020C-45s

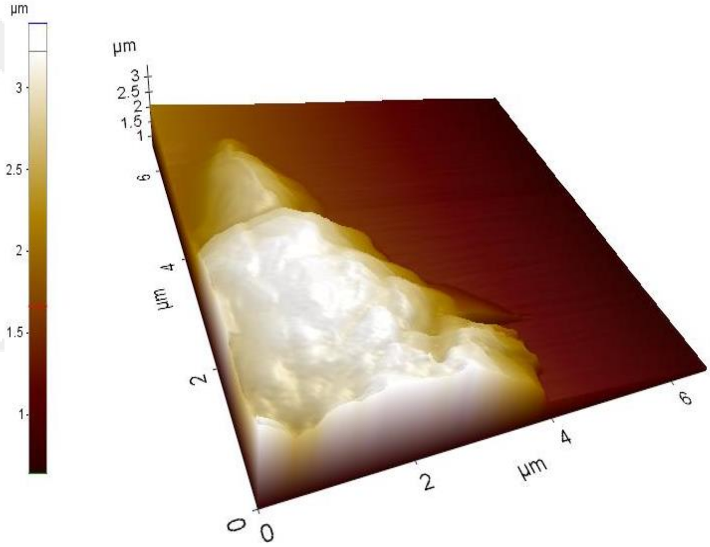

Figure 4.21 : AFM profile of 1050C-35s

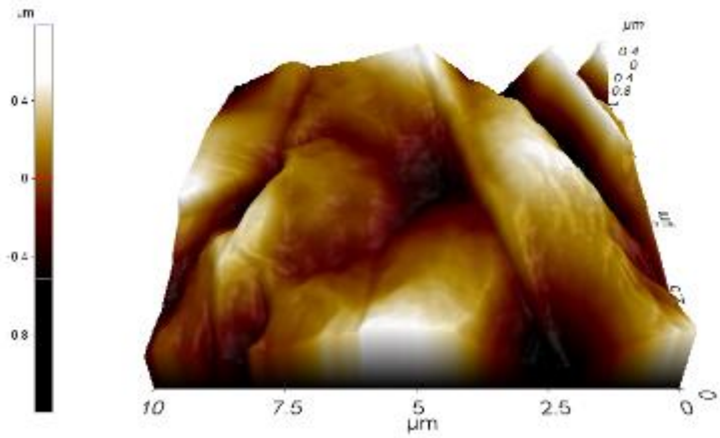

Figure 4.22 : AFM profile of 1020C-35s

4.7 X-ray Diffraction (XRD)

When the crystal structure of the fibers in Table 4.7 is examined by XRD results, the crystallinity level decreased for 1000C-35s compared to 1050C-15s the crystal size increased and the distance between the layers decreased and the number of layers increased. As can be seen from the XRD analysis results, at the same temperature, when the percentage of crystallinity is decreased as the time is increased, the crystal sizes present are increased, therefore crystal package size is increased. When the temperature increased from 1000^{o}C to 1050^{o}C, better exfoliation occurred between the layers, and the crystal grades also increased, resulting in a more regular package. According to the results, as the temperature increases, the crystal size and the distance between layers decrease, but the distance between the layers, the number of layers, the crystal level and the crystal size increase. Ultrasonication causes the functional groups in the structure to break. At sample 1020C-45s crystallinity degree was higher than sample 1020C-35s but d space of sample was lower. The circumstance can be explained with reduction of higher degree of carbon. It can be seen also from C/O ratio values.

Table 4.7 : XRD results of samples

Samples	% Crystallinity	Crystalline size (Å)	d_{hkl}	Number of layers
1000C-15s	78.1	542.6	6.73	84.34
1000C-35s	65.4	605	4.92	136.20
1000C-35s-Ult-S	80.9	1029	5.14	293.09
1000C-35s-Ult-L	63.9	3486.5	3.52	1218
1020C-45s	88.2	402	3.33	120.57
1050C-35s	73.9	439	5.72	84.5
1020-35s	40.9	38	7.52	5

5. CONCLUSION

Several parameters have been changed during the exfoliation process such as, temperature and time. Hummers method is an efficient method for synthesis of GO. Therefore, Hummers method was used before homogenization step. Then graphene oxide fibers were obtained by wet spinning method. Fibers can find application areas such as filter, wearable electronics, batteries, sensors, which were produced via wet-spinning and coagulation technique. Characterization of GO fibers were performed by SEM, AFM, XPS, XRD, tensile testing and conductivity testing.

Because of the changing of production parameters, different results were obtained. For instance; when higher exfoliation time was used, Tex count of fiber increased. Exfoliation temperature had slight effect on Tex count of fiber when it was increased from 1000°C to 1050 °C. The crystal size and number of layers were also affected from exfoliation time.

Other additional step was ultrasonication and longer time of ultrasonication caused to lower Tex value of the GO fiber compared to both shorter ultrasound time and mechanical homogenization. Breakage of chains resulted to this situation with long ultrasonication.

Homogenization techniques were also important parameter for fiber properties. Crystaline size and number of layers were affected by this parameter. Increasing of ultrasonication time caused to decrease of crystallinity degree and d-space together. But it caused to increase crystalline size and number of layers. The circumstance can be explained by shear force and pressure during wet spinning.

The structural analyses of GO fibers which were obtained by SEM showed difference of surface roughness. When exfoliation time were increased, it caused higher expansion and it resulted less rough surface on fiber. CS images of fibers showed more flattened flakes and it was the cause of decrease in surface roughness.

Defects and voids can be observed because of exfoliation at high temperature. This situation increased surface roughness. Furthermore, by enhancing of ultrasonication time from 15 min to 60 min, reduction of surface roughness was observed. Because of sonic waves, flake sizes were getting smaller.

According to XPS results, C/O ratio of samples were obtained. C/O ratio decreased when longer ultrasonication and higher exfoliation temperatures were applied. Contrariwise, percentage of oxygen increased with longer ultrasonic time. C/O ratio is important, because it gives an idea about conductivity.

Many parameters can affect electrical conductivity. These were also examined in this study and it was seen that C/O ratio, morphological properties and electrical networks had vital effect on condutivity properties. Higher electrical conductivity were obtained when shorter ultrasonication period was obtained compared with mechanical homogenization and longer ultrasonication. Better electrical networks can be obtained when longer ultrasonication was applied. Due to this network electrical conductivity improved. Normally it was expected that higher C/O ratio for longer ultrasonication. Because electrical conductivity was better than shorter one. But, longer ultrasonification period showed a high electrical conductivity although it had the lowest C/O ratio. Smaller flakes can be played an important role in this situation. Flakes filled the gaps along the conductivity path and gave the sample better conductivity properties. Temperature of exfoliation did not have significant effect on the fiber conductivity.

It is known that mechanical properties have important for fiber characteristics. Breaking strenth and elongation asre affected from orientation, uniformity morphology and many other parameters. According to the experimets which were performed for this study, higher exfoliation temperature showed better mechanical properties. It has been found that the 1050C-35s, 1020C-45s, 1020C-35s provide relatively better mechanical properties.

When we compared ultrasonic treatment and mechanical homogenisation, it is observed that ultrasonication gave better mechanical properties at same temperatures. It can be explained with better homogenisation of GO flakes in dispersion.

By the addition of activated carbon in dispersion, it was not observed any improve on mechanical properties. It had negative effect on fiber properties. According to visual examinations by SEM, it can be seen that fibers with AC had rough structure. Because of fiber’s harsh and porous structure, mechanical properties and electrical conductivity got worse.

In the light of this study, optimal conditions for producing continuous graphene oxide fibers can be determined. This study can take an important role for further researches.

REFERENCES

[1] Qin Y., (2016). *Medical Textile Materials: A volume in Woodhead Publishing, Series in Textiles, A brief description of textile fibers*, United Kingdom: Elsevier (pp. 23-42).

[2] Miao M. and Gordon S. *Engineering of High-Performance Textiles: A volume in The Textile Institute Book Series, Fiber selection and substitution* , United Kingdom: Elsevier (pp. 3-26).

[3] Miller G. C., Yu J., Joseph R.M., Choudhury S.R., Mecham S.J., Baird D.G., Bortner M., Norris R.E., Paulauskas F.L., Riffle J.S., (2017) Melt-spinnable polyacrylonitrile copolymer precursors for carbon fibers, *Polymer*, 126, 87-95.

[4] Kutlu B., Meinl J., Leuteritz A., Brünig H., Heinrich G. (2013). Melt-spinning of LDH/HDPE nanocomposites, *Polymer*, 54, 5712-5718.

[5] Ding G., Si J., Yang S., Wang G., Wub H. (2016) High thermoelectric properties of n-type Cd-doped PbTe prepared by melt spinning, *Scripta Materialia*, 122, 1–4.

[6] Tomisawa R., Ikaga T., Kim K.H., Ohkoshi Y., Okada K., Masunaga H., Kanaya T., Masuda M., Maeda Y. (2017). *Polymer*,116, 367-377.

[7] Ozipek B. and Karakas H., *Advances in Filament Yarn Spinning of Textiles and Polymers*, Wet spinning of synthetic polymer fibers, United Kingdom: Elsevier (pp. 174-186).

[8] Lin H., Dong H., Xu S., Wang X., Zhang J., Wang Y. (2016). Thermal transportingraphene fiber fabricatedbywet-spinning method, *Materials Letters*, 183, 147–150.

[9] Foroughi J., Spinks G. M., Wallace G. G., Whitten P. G. (2008). Production of polypyrrole fibres by wet spinning, *Synthetic Metals*, 158, 104-107.

[10] Mo M., Chen C., Gao H., Chen M., Li D. (2018). Wet-spinning assembly of cellulose nanofibers reinforced graphene/polypyrrole microfibers for high performance fiber-shaped supercapacitors, *Electrochimica Acta*, 269, 11-20.

[11] Hu X., Li J., Bai Y. (2017). Fabrication of high strength graphene/regenerated silk fibroin composite fibers by wet spinning, *Materials Letters*, 194, 224-226.

[12] Imura Y., Hogan R. M. C., Jaffe. (2014). *Advances in Filament Yarn Spinning of Textiles and Polymers: Dry spinning of synthetic polymer fibers*, United Kingdom: Woodhead Publishing (pp. 187-202).

[13] Zhang M., Ogale A.A. (2014). Carbon fibers from dry-spinning of acetylated softwood kraft lignin, *Carbon*, 69, 626-629.

[14] Gou Z., McHugh A. J. (2014). Two-dimensional modeling of dry spinning of polymer fibers, *J. Non-Newtonian Fluid Mech*, 118, 121–136.

[15] Park S. K., Farris R. J. (2001). Dry-jet wet spinning of polyamic acid fiber using chemical imidization, *Polymer,* 42, 10087-10093.

[16] Kim D. B., Lee Y. M., Lee W. S., Jo S. M., Kim B. C. (2002). Double crystallization behavior in dry-jet wet spinning of cellulose/N-methylmorpholine-N-oxide hydrate solutions, *European Polymer Journal*, 38, 109-119.

[17] Kuo C. J., Lan W. L. (2014). *Advances in Filament Yarn Spinning of Textiles and Polymers*, *Gel spinning of synthetic polymer fibres,* United Kingdom: Woodhead Publishing (pp. 100-112).

[18] Tan L., Wan A., Pan D. (2011). Pregelled gel spinning of polyacrylonitrile precursor fiber, *Materials Letters*, 65, 887–890.

[19] Zhang X., Liu T., Sreekumar T.V., Kumar S., Hu X., Smith S. (2004). Gel spinning of PVA/SWNT composite fiber, *Polymer*, 45, 8801–8807.

[20] Ni Q. Q., Jin X. D., Xia H., Liu F. (2004). *Advances in Filament Yarn Spinning of Textiles and Polymers*, *Electrospinning, processing and characterization of polymer-based nano-composite fibers*, United Kingdom: Woodhead Publishing (pp. 128-148).

[21] Bhardwaj N., Kundu S. C. (2010). Electrospinning: A fascinating fiber fabrication technique, *Biotechnology Advances*, 28, 325–347.

[22] Wei Y., Zhang L., Gong C., Liu S., Zhang M., Shi Y., Zhang J. (2018). Fabrication of TiN/Carbon nanofibers by electrospinning and their electromagnetic wave absorption properties, *Journal of Alloys and Compounds*, 735, 1488-1493.

[23] Dincer K., Waisi B., Önal G., Tuğluoğlu N., McCutcheon J., Yüksel Ö.F. (2018). Investigation of optical and dispersion parameters of electrospinning grown activated carbon nanofiber (ACNF) layer, *Synthetic Metals*, 237, 16–22.

[24] Chinnappan A., Lee J. K. Y., Jayathilaka W.A.D.M., Ramakrishna S. (2018). Fabrication of MWCNT/Cu nanofibers via electrospinning method and analysis of their electrical conductivity by four-probe method, *International Journal of Hydrogen Energy*, 43, 721-729.

[25] Uçar N., Ölmez M., Alptoğa Ö., Yavuz N., Önen A. (2016). Graphene oxide fiber with different exfoliation time and cctivated carbon particle, *World Academy of Science*, 12, 1514-1518.

[26] Novoselov K. S., Geim A. K., Morozov S. V., Jiang D., Zhang Y., Dubonos S. V., Grigorieva I. V., Firsov A. A. (2004). Electric field effect in atomically thin carbon film**,** *Science***,** 306, 666.

[27] Phiri J., Gane P., Maloney T. C. (2017). General overview of graphene: Production, properties and application in polymer composites**,** *Materials Science and Engineering*, B 215, 9–28.

[28] Han T. H., Kim H., Kwon S. J., Lee T. W. (2017). Graphene-based flexible electronic devices**,** *Materials Science and Engineering*, R 118, 1–43.

[29] Lee C., Wei X., Kysar J. W., Hone J. (2008). Measurement of the elastic properties and intrinsic strength of monolayer graphene, *Science*, 321, 385–388.

[30] Dikin D. A., Stankovich S., Zimney E. J., Piner R. D., Dommett G. H. B., Evmenenko G., Nguyen S. T., Ruoff R. S. (2007). Preparation and characterization of graphene oxide paper**,** *Nature***,** 448, 457–460.

[31] Chu K., Wang X, Li Y., Huang D., Geng Z., Zhao X., Liu H., Zhangb H. (2018). Thermal properties of graphene/metal composites with aligned graphene**,** *Materials and Design,* 140, 85–94.

[32] Wang T., Yu J., Wang M., Cao Y., Dai W., Shen D., Guo L., Wu Y., Bai H., Dai D., Lyu J., Jiang N., Pan C., Lin C. (2017). Effect of different sizes of graphene on thermal transport performance of graphene paper**,** *Composites Communications*, 5, 46–53.

[33] Xu Z., Gao C. (2015). Graphene fiber: a new trend in carbon fibers**,** *Materials Today***,** 18, 480-492.

[34] Paulchamy B., Arthi G., Lignesh B.D. (2015). A Simple approach to stepwise synthesis of graphene oxide nanomaterial**,** J Nanomed Nanotechnol, 6, No: 253. doi: 10.4172/2157-7439.1000253.

[35] Huang X., Qui X., Boey F., Zhang H. (2012). Graphene-based composites**,** *Chem. Soc. Rev*, 41, pp. 666–686.

[36] Fan T., Zhao C., Xiao Z., Guo F., Cai K., Lin H., Liu Y., Meng H., Min Y., and Epstein A. J. (2016). Fabricating of high-performance functional graphene fibers for micro-capacitive energy storage, *Scientific Reports***,** 6, 1-8.

[37] Cong H.P., Ren, X.C., Wang, P., Yu, S.H., (2012). Wet-spinning assembly of continuous, neat, and macroscopic graphene fibers**,** *Scientific Reports,* 2, 1-6.

[38] Chen Z., Zhou X., Wang X., Guo P. (2018). Mechanical behavior of multilayer GO carbon-fiber cement composites**,** *Construction and Building Materials,* 159, 205-212.

[39] Mazzoli A., Corinaldesi V., Donnini J., Di Perna C., Micheli D., Vricella A., Pastore R., Bastianelli L., Moglie F., Mariani Primiani V. (2018). Effect of graphene oxide and metallic fibers on the electromagnetic shielding effect of engineered cementitious composites**,** *Journal of Building Engineering,* 18, 33–39.

[40] Terasawa N., Asaka K. (2018). High-performance graphene oxide/vapor-grown carbon fibercomposite polymer actuator**,** *Sensors and Actuators,* B 255, 2829–2837.

[41] Fancheng M., Wang M., Lu W., Li Q., Chou T. W., Zheng L. (2016). An electromechanical behavior of reduced graphene oxide fiber**,** *Carbon,* 105, 244-247.

[42] Ucar N., Gokceli G., Yuksek I. O., Onen A., and Karatepe Yavuz N. (2016) Graphene oxide and graphene fiber produced by different nozzle size, feed rate and reduction time with vitamin C**.** *J. Ind. Tex.*

[43] Huang T., Zheng B., Kou L., Gopalsamy K., Xu Z., Gao C., Meng Y., and Mei Z. (2013). Flexible high performance wet-spun graphene fiber supercapacitors**.** *RSC Adv***.,** 3(46), 23957–23962.

[44] He Y., Zhang N., Gonga Q., Qiu H., Wang W., Liu Y., and Gao J. (2012). Alginate/graphene oxide fibers with enhanced mechanical strength prepared by wet spinning**,** *Carbohydr. Polym***.,** 88(3), 1100–1108.

[45] Ma W., Chena S., Yang S., Chen W., Cheng Y., Guo Y., Peng S., Ramakrishna S., and Zhu M. (2016)**.** Hierarchical MnO2 nanowire/graphene hybrid fibers with excellent electrochemical performance for flexible solid-state supercapacitors**,** *J. Power Sources***,** 306, 481–488.

[46] Zhang J., Cao Y., Qiao M., Ai L., Sun K., Mi Q., Zang S., Zuo Y., Yuan X., Wang Q., (2018)**.** Human motion monitoring in sports using wearable graphene-coatedfiber sensors**,** *Sensors and Actuators*, A 274, 132–140.

[47] Li Y., Sun J., Du Q., Zhang L., Yang X., Wu S., Xia Y., Wang Z., Xia L., Cao A. (2014)**.** Mechanical and dye adsorption properties of graphene oxide/chitosancomposite fibers prepared by wet spinning**,** *Carbohydrate Polymers*, 102, 755–761.

[48] Gao R., Lu D., Cheng J., Jiang Y., Jiang L., Qi Z. (2016)**.** Humidity sensor based on power leakage at resonance wavelengths ofa hollow core fiber coated with reduced graphene oxide**,** *Sensors and Actuators*, B 222, 618–624.

[49] Xiong C., Li T., Zhao T., Dang A., Li H., Ji X., Jin W., Jiao S., Shang Y., Zhang Y. (2017). Reduced graphene oxide-carbon nanotube grown on carbon fiber as binder-free electrode for flexible high-performance fiber supercapacitors**,** *Composites Part*, B 116, 7-15.

[50] Jalili R., Aboutalebi S., and Esrafilzadeh D. (2013). Scalable one-step wet-spinning of graphene fibers and yarns from liquid crystalline dispersions of graphene oxide: Towards multifunctional textiles**.** *Adv. Funct. Mater.*, 43(23), 5345–5354.

[51] Hummers W. S., & Offeman R. E. (1958). Preparation of graphitic oxide. *Journal of the American Chemical Society*, 80, 1339–1339. doi:10.1021/ ja01539a017.

[52] McAllister M. J., Li J. L., Adamson D. H., Schniepp H. C., Abdala A. A., Liu J., Herrera-Alonso M., Milius D. L., Car R., Prud'homme R. K., Aksay I. A. (2007). Single Sheet Functionalized Graphene by Oxidation and Thermal Expansion of Graphite**,** *Chem. Mater***.,** 19, 4396-4404.

[53] Zhang C., Wei L., Xie X., Tang D., Liu C., Yang Q. H. (2013) Towards low temperature thermal exfoliation of graphite oxide for graphene production**,** *Carbon***,** 62, 11–24.

[54] Zhang X., Song X. H., Zhang D. L. (2010). Thickness dependence of grain size and surface roughness for dc magnetron sputtered Au films, *Chin. Phys.* B 19, No. 8 086802.

[55] Yu R., Jiang C. F., Chu W., Ran M. F., Sun W. J., (2016). Decoration of CNTs' surface by Fe3O4 nanoparticles: Influence of ultrasonication time on the magnetic and structural properties**,** *Chinese Chemical Letters.*

[56] Madras G., Kumar S., Chattopadhyay S., (2000). Continuous distribution kinetics for ultrasonic degradation of polymers**,** *Polymer Degradation and Stability*, 69, 73-78.

[57] Zhang L., Ye X., Ding T., Sun X., Xu Y., Liu D., (2013). Ultrasound effects on the degradation kinetics, structure and rheological properties of apple pectin, *Ultrasonics Sonochemistry***,** 20, 222–231.

[58] Kardos N., Luche J. L. (2001). Sonochemistry of carbohydrate compounds**,** *Carbohydrate Research,* 332, 115–131.

[59] Parvez K., Yang S., Feng X. , Müllen K., (2015). Exfoliation of graphene via wet chemical routes, Synthetic Metals**,** *Synthetic Metals*, 210, 123–132.

[60] Chia J. S. Y., Tan M. T.T., Khiew P. S., Chin J. K., Lee H., Bien D. C. S., Teh A. S., Siong C. W. (2013). Facile synthesis of few-layer graphene by mild solvent thermal exfoliation of highly oriented pyrolytic graphite, *Chemical Engineering Journal,* 231, 1–11.

[61] Konios D., Stylianakis M. M., Stratakis E., Kymakis E. (2014). Dispersion behaviour of graphene oxide and reduced graphene oxide, *Journal of Colloid and Interface Science***,** 430, 108–112.

[62] Johnson D. W., Dobson B. P., Coleman K. S. (2015). A manufacturing perspective on graphene dispersions, *Current Opinion in Colloid & Interface Science,* 20, 367–382.

[63] Texter J. (2014). Graphene dispersions**, *Current Opinion in Colloid & Interface Science,*** 19, 163–174.

[64] Dintcheva N. T., Arrigo R., Teresi R., Megna B., Gambarotti C., Marullo S., D'Anna F. (2016). Tunable radical scavenging activity of carbon nanotubes through sonication**,** *Carbon*, 107, 240–247.

[65] Koshio A., Yudasaka M., Zhang M., Iijima S. (2001). A Simple Way to Chemically React Single-Wall Carbon Nanotubes with Organic Materials Using Ultrasonication, *Nano Letters,* 1, No. 7 361-363.

[66] Kizildag, N., Ucar, N. (2016). Investigation of the properties of PAN/f-MWCNTs/AgNPs composite nanofibers**, *Jo*urnal *of Industrial Textiles.***

[67] Kizildag N., Ucar N., Onen A., Karacan I. (2016). Polyacrylonitrile/polyaniline composite nanofiber webs with electrostatic discharge properties**,** *Journal of Composite Materials***,** DOI: 10.1177/0021998316630583.

[68] Ucar N., Kizildag N., Onen A, Karacan I, Eren O. (2015). Polyacrylonitrile-polyaniline Composite Nanofiber Webs: Effects of Solvents, Redoping Process and Dispersion Technique, *Fibers and Polymers,* 16(10), 2223-2236, DOI: 10.1007/s12221-015-5426-3.

[68] Demirsoy N., Ucar N., Onen A., Karacan I., Kizildag N., Eren O., Borazan I. (2014). The effect of dispersion technique, silver particle loading, and reduction method on the properties of polyacrylonitrile−silver omposite nanofiber, Journal of Industrial Textiles, DOI: 10.1177/1528083714553690.

CURRICULUM VITAE

Name Surname : **Mervin ÖLMEZ**

Place and Date of Birth : **Şişli – 15.10.1992**

E-Mail : **mervinolmez@gmail.com**

EDUCATION

- **B.Sc.** : 2016, Istanbul University, Faculty of Engineering, Chemical Engineering Department

PUBLICATIONS, PRESENTATIONS AND PATENTS ON THE THESIS:

- **Olmez M., Ucar N., Can E., Onen A., Yavuz N. K.** 2016: The Effect of Production Parameters on Continuous Graphene Oxide Fiber. 13th International Nanoscience and Nanotechnologies Conference, July 5-8, 2016, Thessaloniki, Greece.
- **Olmez M., Ucar N., Can E., Onen A., Mehmedi Z., Yavuz N. K.** 2016: Continuous Graphene Oxide Fiber. 12th International Nanoscience and Nanotechnology Conference, June 3-5, 2016, Gebze, Turkey
- **Ucar N., Olmez M., Alptoga Ö., Yavuz N. K. & Onen A.** (2016). Graphene Oxide Fiber with Different Exfoliation Time and Activated Carbon Particle, *World Academy Science Engineering and Technology*, 1514-1518
- **Ucar N., Can E., Yuksek I.O., Olmez M., Onen A., Yavuz N. K.** (2017). The effect of exfoliation and plasma application on the properties of continuous graphene oxide fiber, *Fullerenes, Nanotubes and Carbon Nanostructures*, 25:10, 570-575,
- **Ucar N., Olmez M., Kayaoğlu B., Onen A., Yavuz N. K. & Eksik O.** (2018). Structural properties of graphene oxide fibers: from graphene oxide dispersion until continuous graphene oxide fiber, *The Journal of the Textile Institute*, DOI: 10.1080/00405000.2018.1454088